INDUSTRIALES
ETSII | UPM

E.T.S. Ingenieros Industriales
Universidad Politécnica de Madrid

Ideas to create an adaptive finite element method for combustion problems

Jaime Carpio Huertas

A jointly work with:

Professors:
Rodolfo Bermejo
Marcos Vera
Miguel Hermanns
Amable Liñán

Students:
Pablo Fraile
Ángel Fernández

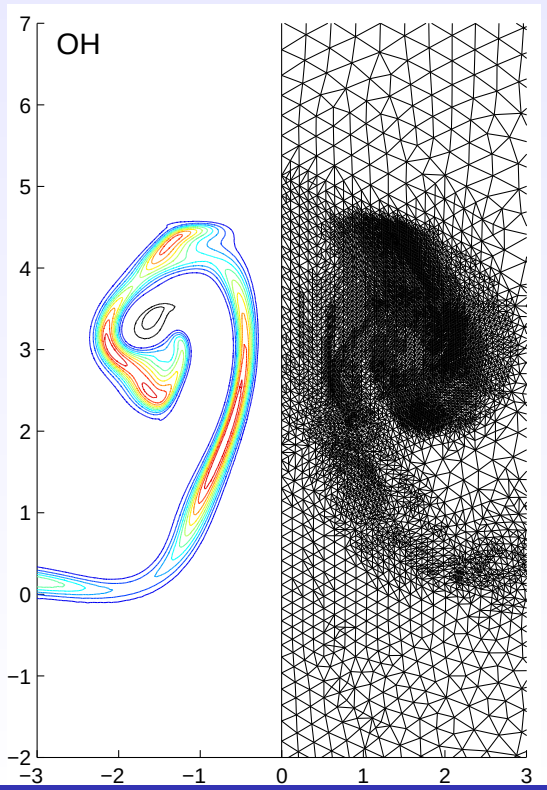

Workshop on mathematical modelling of combustion
23-25/05/2011

Outline

1. Physical phenomenon
2. Model I
   - Mathematical model
   - Numerical method
   - Refinement strategies
3. Model II
   - Mathematical model
   - Numerical validation
4. Conclusions

(Loading...)

Physical phenomenon: Diffusion-Flame/Vortex Interactions

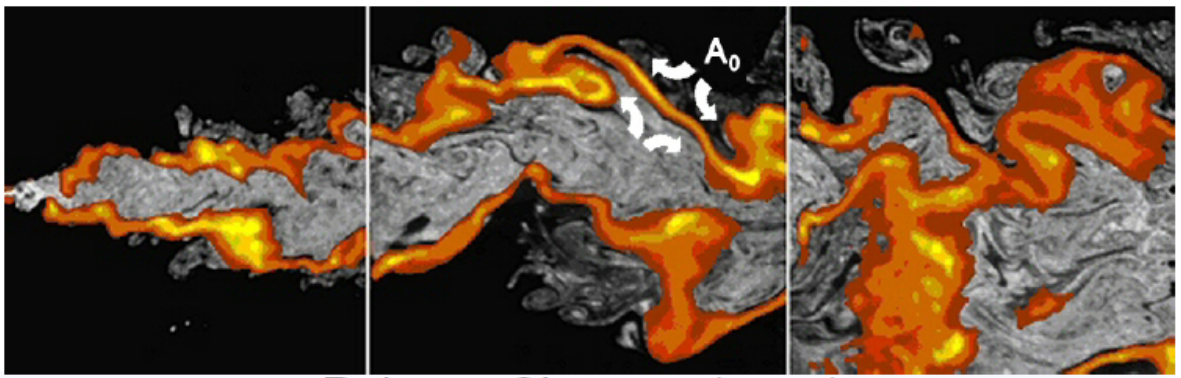

Rehm & Clemens (1997)

- Turbulent combustion occurs in the form of laminar flames embedded in thin mixing layers locally strained by vortices.

Physical phenomenon: Diffusion-Flame/Vortex Interactions

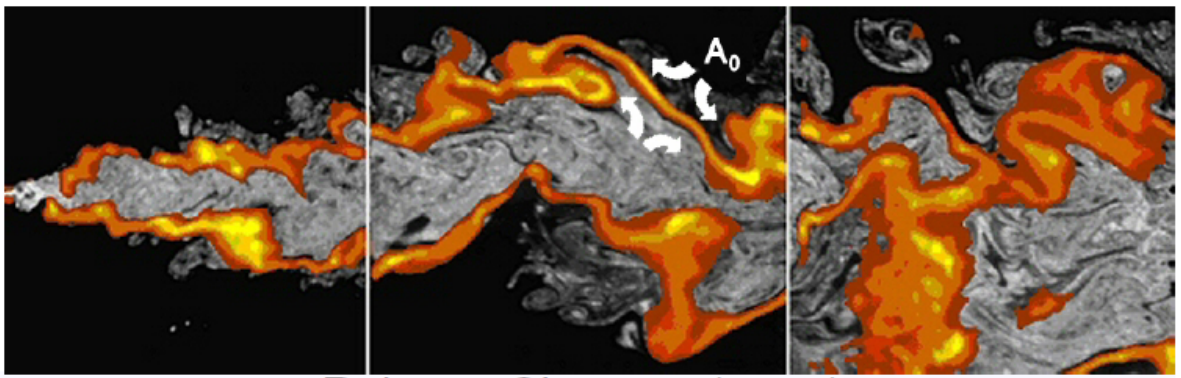

Rehm & Clemens (1997)

- Turbulent combustion occurs in the form of laminar flames embedded in thin mixing layers locally strained by vortices.

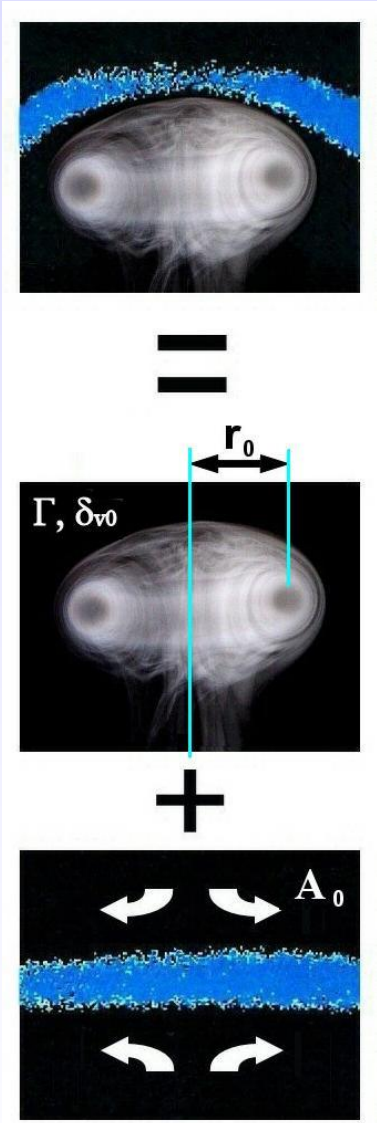

Physical phenomenon: Diffusion-Flame/Vortex Interactions

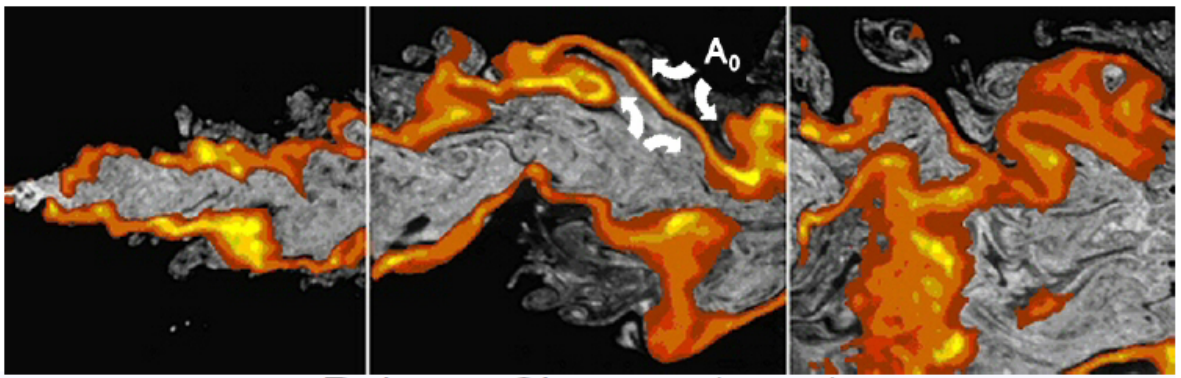

Rehm & Clemens (1997)

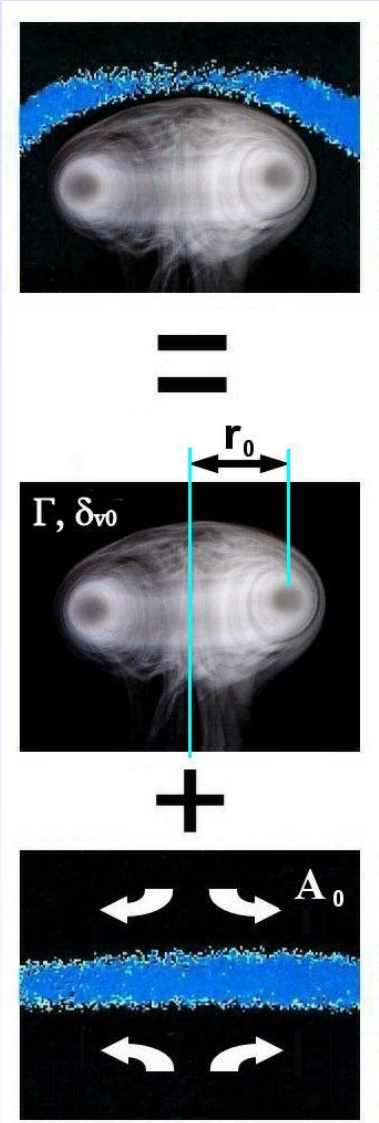

- Turbulent combustion occurs in the form of laminar flames embedded in thin mixing layers locally strained by vortices.
- A complete description of the phenomenon requires:
  - a good mathematical model.
  - an efficient numerical method.

Physical phenomenon: Conservation Equations

$$\frac{\partial \rho}{\partial \tau} + \nabla \cdot (\rho \mathbf{u}) = 0$$

$$\rho \left(\frac{\partial \mathbf{u}}{\partial \tau} + (\mathbf{u} \cdot \nabla)\mathbf{u} \right) = -\nabla p + \frac{Pr}{Pe_0} \nabla \cdot \left[\mu \left(\nabla \mathbf{u} + \nabla \mathbf{u}^{\mathrm{T}} \right) \right]$$

$$\rho \left(\frac{\partial h}{\partial \tau} + \mathbf{u} \cdot \nabla h \right) = \frac{1}{Pe_0} \nabla \cdot \mathbf{q}$$

$$\rho \left(\frac{\partial Y_i}{\partial \tau} + \mathbf{u} \cdot \nabla Y_i \right) = \frac{1}{Pe_0} \nabla \cdot \mathbf{j}_i + \mathcal{R} \dot{m}_i \qquad i \neq N_2$$

Scales

$$r_0, A_0, \rho_A, D_{TA}, h_A, \mu_A$$

Dimensionless parameters

$$Pe_0 = \frac{A_0 r_0^2}{D_{TA}}, \quad \mathcal{R} = \frac{A_{ext}}{A_0}, \quad \widetilde{\Gamma} = \Gamma / \left(2 A_0 r_0^2 \right), \quad Pr = 0.72$$

Model I

- Model I (Simple model)
  - Constant fluid properties.
  - Infinitely fast chemical reaction.

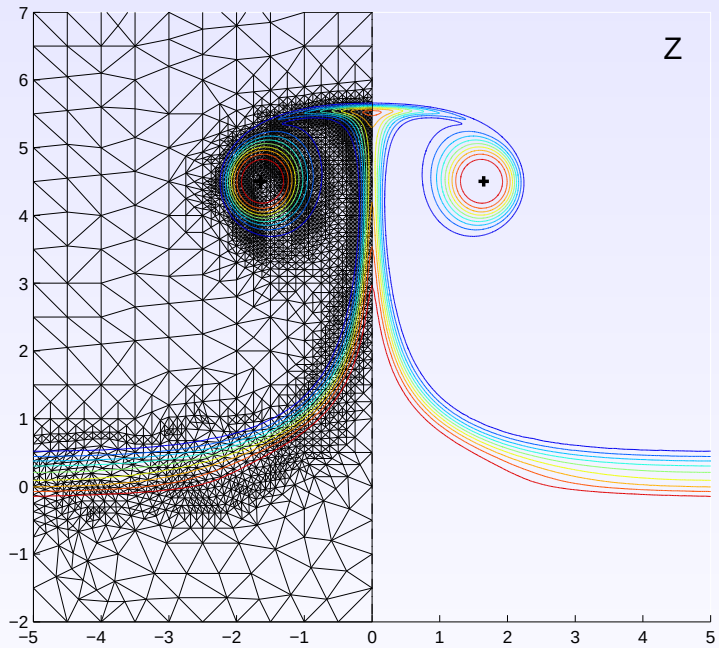

Model I: Constitutive Equations

- Molecular transport models

$\mathbf{j}_i = \rho D_i Y_i.$

$\mathbf{q} = -\lambda \nabla T + \sum_{i=1}^{I} h_i \mathbf{j}_i,$

with $\rho = \dfrac{\rho'}{\rho_A} = 1, \quad \mu = \dfrac{\mu'}{\mu_A} = 1, \quad \lambda = \dfrac{\lambda'}{\rho_A D_{TA} Cp_A} = 1, \quad \rho D_i = \dfrac{\rho' D_i'}{\rho D_{TA}} = 1.$

and $h_i = h_i'/h_A, \qquad h_i' = {h'}_i^0 + Cp_A(T' - T_0)$

Model I: Constitutive Equations

- Molecular transport models

  $\mathbf{j}_i = \rho D_i Y_i.$

  $\mathbf{q} = -\lambda \nabla T + \sum_{i=1}^{I} h_i \mathbf{j}_i,$

  with $\rho = \dfrac{\rho'}{\rho_A} = 1, \quad \mu = \dfrac{\mu'}{\mu_A} = 1, \quad \lambda = \dfrac{\lambda'}{\rho_A D_{TA} Cp_A} = 1, \quad \rho D_i = \dfrac{\rho' D_i'}{\rho D_{TA}} = 1.$

  and $h_i = h_i'/h_A, \qquad h_i' = {h'}_i^0 + Cp_A(T' - T_0)$

- The chemical reaction is assumed to be infinitely fast:

$$F + sO_2 \rightarrow (1+s)P \quad + \quad q\left(\sum_{i=1}^{I} \nu_i h_i\right) \qquad \mathcal{R} \rightarrow \infty$$

Model I: Constitutive Equations

- Molecular transport models

  $\mathbf{j}_i = \rho D_i Y_i.$

  $\mathbf{q} = -\lambda \nabla T + \sum_{i=1}^{I} h_i \mathbf{j}_i,$

  with $\rho = \dfrac{\rho'}{\rho_A} = 1, \quad \mu = \dfrac{\mu'}{\mu_A} = 1, \quad \lambda = \dfrac{\lambda'}{\rho_A D_{TA} Cp_A} = 1, \quad \rho D_i = \dfrac{\rho' D_i'}{\rho D_{TA}} = 1.$

  and $h_i = h_i'/h_A, \qquad h_i' = {h'}_i^0 + Cp_A(T' - T_0)$

- The chemical reaction is assumed to be infinitely fast:

$$F + sO_2 \rightarrow (1+s)P \quad + \quad q\left(\sum_{i=1}^{I} \nu_i h_i\right) \qquad \mathcal{R} \rightarrow \infty$$

- Energy and mass fraction equations introduce the mixture fraction Z defined as:

$$Z = \frac{SY_F/Y_{F,0} - Y_{O_2}/Y_{O_2,A} + 1}{1+S} : \qquad \left(\frac{\partial Z}{\partial \tau} + \mathbf{u} \cdot \nabla Z\right) = \frac{1}{Pe_0} \Delta Z$$

Model I: Original variables

- Z allows us to define the temperature, mass fractions of oxygen and fuel:

$$T = 1 + \gamma\left(\frac{1-Z}{1-Z_s}\right), \quad \frac{Y_F}{Y_{F,0}} = \frac{1-Z}{1-Z_s}, \quad Y_{O_2} = 0 \qquad \text{if } Z \geq Z_S$$

$$T = 1 + \gamma\frac{Z}{Z_s}, \qquad Y_F = 0, \qquad \frac{Y_{O_2}}{Y_{O_2,A}} = 1 - \frac{Z}{Z_s} \qquad \text{if } Z < Z_S$$

with $Z_S = \dfrac{1}{S+1}$, $S = \dfrac{sY_{F,0}}{Y_{O_2,A}}$ and $\gamma = \dfrac{qY_{F,0}}{Cp_A T_0(1+S)}$

Model I: Original variables

- Z allows us to define the temperature, mass fractions of oxygen and fuel:

$$T = 1 + \gamma\left(\frac{1-Z}{1-Z_s}\right), \quad \frac{Y_F}{Y_{F,0}} = \frac{1-Z}{1-Z_s}, \quad Y_{O_2} = 0 \qquad \text{if } Z \geq Z_S$$

$$T = 1 + \gamma\frac{Z}{Z_s}, \qquad Y_F = 0, \qquad \frac{Y_{O_2}}{Y_{O_2,A}} = 1 - \frac{Z}{Z_s} \qquad \text{if } Z < Z_S$$

with $Z_S = \dfrac{1}{S+1}$, $S = \dfrac{sY_{F,0}}{Y_{O_2,A}}$ and $\gamma = \dfrac{qY_{F,0}}{Cp_A T_0(1+S)}$

- The velocity field is given by the incompressible Navier-Stokes equation, which can be to consider known for $Pe \gg 1$

$$u = \xi/2$$

$$v = -\eta$$

Model I: Original variables

- Z allows us to define the temperature, mass fractions of oxygen and fuel:

$$T = 1 + \gamma\left(\frac{1-Z}{1-Z_s}\right), \quad \frac{Y_F}{Y_{F,0}} = \frac{1-Z}{1-Z_s}, \quad Y_{O_2} = 0 \qquad \text{if } Z \geq Z_S$$

$$T = 1 + \gamma\frac{Z}{Z_s}, \qquad Y_F = 0, \qquad \frac{Y_{O_2}}{Y_{O_2,A}} = 1 - \frac{Z}{Z_s} \qquad \text{if } Z < Z_S$$

with $Z_S = \dfrac{1}{S+1}$, $S = \dfrac{sY_{F,0}}{Y_{O_2,A}}$ and $\gamma = \dfrac{qY_{F,0}}{Cp_A T_0(1+S)}$

- The velocity field is given by the incompressible Navier-Stokes equation, which can be to consider known for $Pe \gg 1$

$$u = \xi/2 - \frac{\widetilde{\Gamma}}{\pi\xi_c}\left(\frac{\xi_c}{2\xi}\right)^{3/2}\left(\frac{\eta-\eta_c}{\xi_c}\right) I_1(\mu)\left[1 - \mathrm{e}^{-(\rho/\delta_v)^2}\right]$$

$$v = -\eta + \frac{\widetilde{\Gamma}}{\pi\xi_c}\left(\frac{\xi_c}{2\xi}\right)^{3/2}\left[\frac{\xi}{\xi_c} I_1(\mu) - I_0(\mu)\right]\left[1 - \mathrm{e}^{-(\rho/\delta_v)^2}\right]$$

Hermanns et al., Combustion & Flame (2007)

Model I: Problem to solve

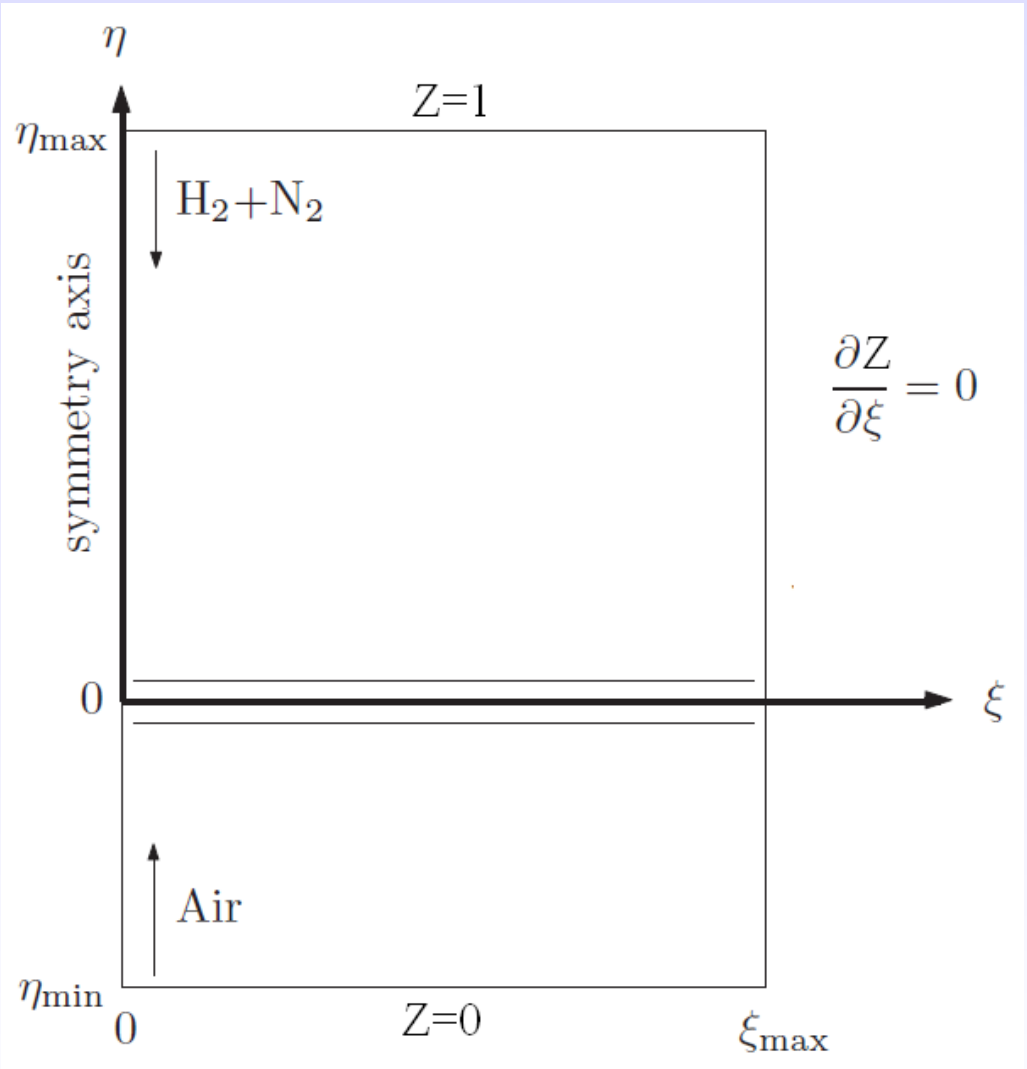

$$\left(\frac{\partial Z}{\partial \tau} + \mathbf{u} \cdot \nabla Z\right) = \frac{1}{Pe_0} \Delta Z$$

Initial condition:

$$Z_0 = 1 - \frac{1}{2} erfc\left[(Pe_0/2)^{1/2}\eta\right]$$

Boundary condition:

Model I: Numerical method

- An efficient numerical treatment of multi-scales phenomena can be carried out with an adaptive method
- The idea is to adapt the domain of integration to the evolving features of the solution

Model I: Numerical method

- An efficient numerical treatment of multi-scales phenomena can be carried out with an adaptive method
- The idea is to adapt the domain of integration to the evolving features of the solution

Model I: Numerical method

- An efficient numerical treatment of multi-scales phenomena can be carried out with an adaptive method
- The idea is to adapt the domain of integration to the evolving features of the solution

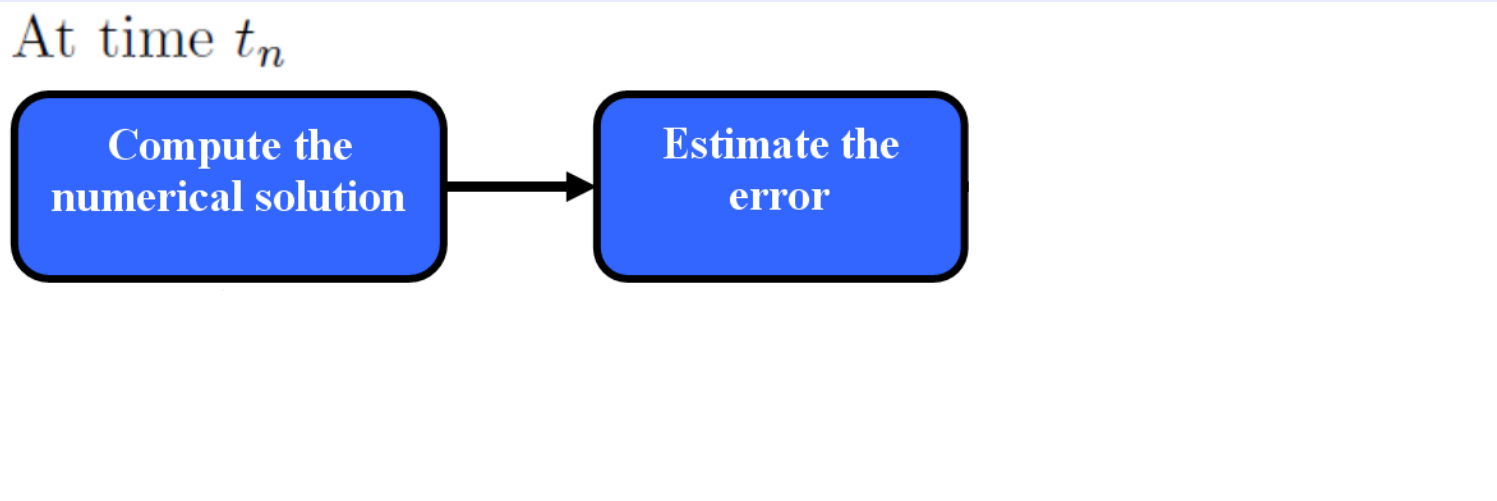

Model I: Numerical method

- An efficient numerical treatment of multi-scales phenomena can be carried out with an adaptive method
- The idea is to adapt the domain of integration to the evolving features of the solution

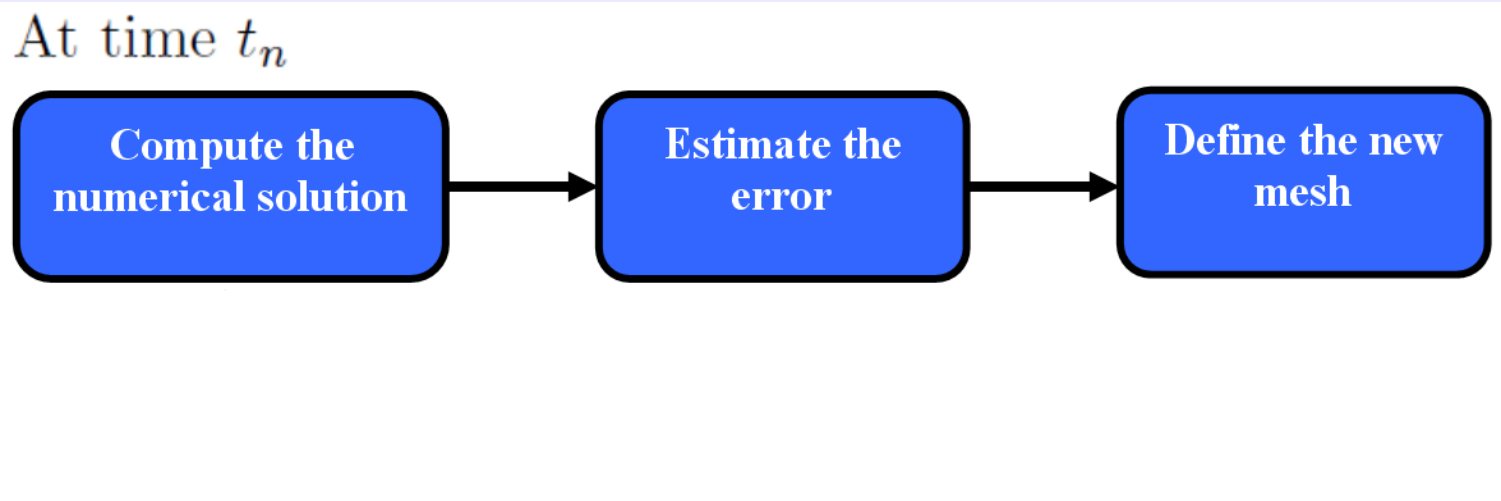

Model I: Numerical method

- An efficient numerical treatment of multi-scales phenomena can be carried out with an adaptive method
- The idea is to adapt the domain of integration to the evolving features of the solution

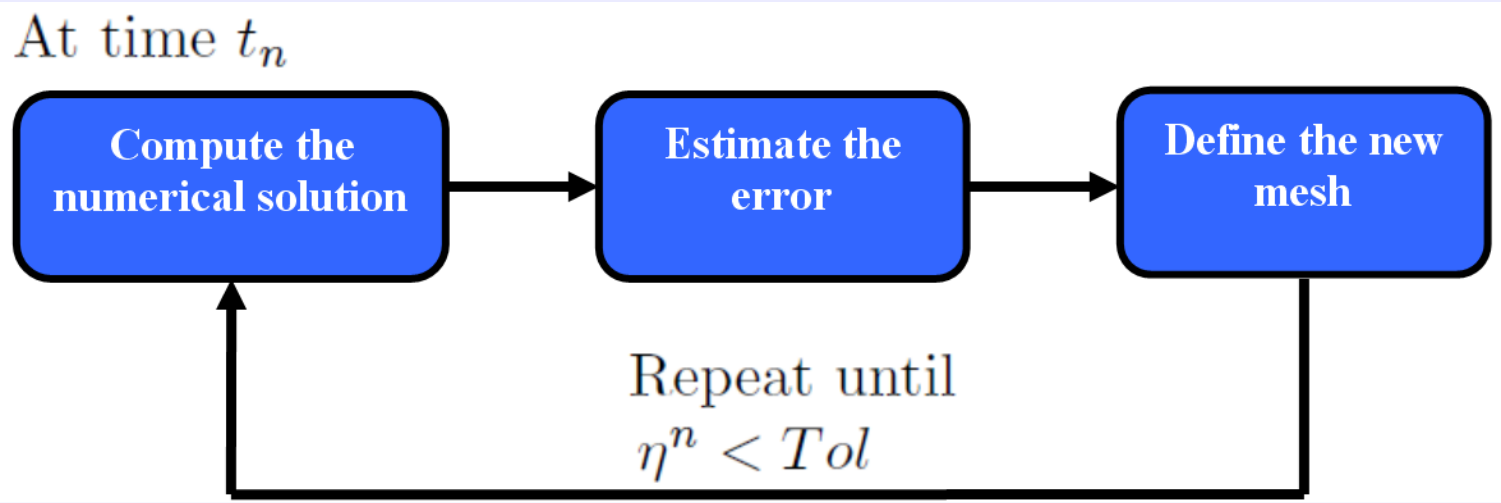

Numerical Method: Compute the numerical solution

- To solve the problem we use a semi-Lagrangian scheme.

$$\left[\frac{\partial Z}{\partial \tau} + \mathbf{u} \cdot \nabla Z = \frac{1}{Pe_0} \Delta Z\right]_{(X(x,\tau_n;\tau),\tau)}$$

$X(x, \tau_n; \tau)$ characteristic curve backwards in time.

Numerical Method: Compute the numerical solution

- To solve the problem we use a semi-Lagrangian scheme.

$$\left[\frac{\partial Z}{\partial \tau} + \mathbf{u}\cdot\nabla Z = \frac{1}{Pe_0}\Delta Z\right]_{(X(x,\tau_n;\tau),\tau)}$$

  $X(x,\tau_n;\tau)$ characteristic curve backwards in time.

- A parabolic equation is obtained

$$\begin{cases} \dfrac{\partial \overline{Z}}{\partial \tau} = \dfrac{1}{Pe_0}\Delta \overline{Z} & \text{in } \left[X\left(x,\tau_n;\tau\right),\tau\right] \text{ with } \tau < \tau_n \\ \overline{Z}_h(x,\tau_{n-1}) \text{ initial condition} \end{cases}$$

  where $\overline{Z}(x,\tau) = Z\left(X(x,\tau_n;\tau),\tau\right)$ and $X\left(x,\tau_n;\tau_n\right) = x$.

Numerical Method: Compute the numerical solution

- To solve the problem we use a semi-Lagrangian scheme.

$$\left[\frac{\partial Z}{\partial \tau} + \mathbf{u}\cdot\nabla Z = \frac{1}{Pe_0}\Delta Z\right]_{(X(x,\tau_n;\tau),\tau)}$$

  $X(x,\tau_n;\tau)$ characteristic curve backwards in time.

- A parabolic equation is obtained

$$\begin{cases} \dfrac{\partial \overline{Z}}{\partial \tau} = \dfrac{1}{Pe_0}\Delta \overline{Z} & \text{in } [X(x,\tau_n;\tau),\tau] \text{ with } \tau < \tau_n \\ \overline{Z}_h(x,\tau_{n-1}) \text{ initial condition} \end{cases}$$

  where $\overline{Z}(x,\tau) = Z(X(x,\tau_n;\tau),\tau)$ and $X(x,\tau_n;\tau_n) = x$.

- Solution:
  1. Convection stage: The aim is calculate $\overline{Z}_h(x,\tau_{n-1})$.
     - Compute $X(x,\tau_n;\tau_{n-1})$ by Runge-Kutta(2).
     - Compute $\overline{Z}_h(x,\tau_{n-1}) \in V_h^n$ (P_2).

  Bermejo & Carpio. IMA Journal of Numerical Analysis (2010).

Numerical Method: Compute the numerical solution

- To solve the problem we use a semi-Lagrangian scheme.

$$\left[\frac{\partial Z}{\partial \tau} + \mathbf{u}\cdot\nabla Z = \frac{1}{Pe_0}\Delta Z\right]_{(X(x,\tau_n;\tau),\tau)}$$

  $X(x,\tau_n;\tau)$ characteristic curve backwards in time.

- A parabolic equation is obtained

$$\begin{cases} \dfrac{\partial \overline{Z}}{\partial \tau} = \dfrac{1}{Pe_0}\Delta \overline{Z} & \text{in } [X(x,\tau_n;\tau),\tau] \text{ with } \tau < \tau_n \\ \overline{Z}_h(x,\tau_{n-1}) \text{ initial condition} \end{cases}$$

  where $\overline{Z}(x,\tau) = Z(X(x,\tau_n;\tau),\tau)$ and $X(x,\tau_n;\tau_n) = x$.

- Solution:
  1. Convection stage: The aim is calculate $\overline{Z}_h(x,\tau_{n-1})$.
     - Compute $X(x,\tau_n;\tau_{n-1})$ by Runge-Kutta(2).
     - Compute $\overline{Z}_h(x,\tau_{n-1}) \in V_h^n$ (P_2).

     Bermejo & Carpio. IMA Journal of Numerical Analysis (2010).
  2. Parabolic part: The aim is calculate $Z_h(x,\tau_n) = \overline{Z}_h(x,\tau_n)$.
     - Crank-Nikolson scheme in time.
     - Quadratic finite element in space.

Numerical Method: Error estimation I

Local a posteriori error will be computed.

- The error in the numerical integration is both in time and in space. However, $\Delta t = 0.005$ and we are only considering spatial adaptation.
- Spatial error can be evaluated as:

$$\eta_s^n = \eta_{conv}^n + \eta_{diff-reac}^n$$

Bermejo & Carpio. Boletín de la Sociedad de Matemática Aplicada (2008).

Numerical Method: Error estimation I

Local a posteriori error will be computed.

- The error in the numerical integration is both in time and in space. However, $\Delta t = 0.005$ and we are only considering spatial adaptation.
- Spatial error can be evaluated as:

$$\eta_s^n = \eta_{conv}^n + \eta_{diff-reac}^n$$

Bermejo & Carpio. Boletín de la Sociedad de Matemática Aplicada (2008).

- For $Pe_0 \gg 1 \longrightarrow \eta_{conv}^n \gg \eta_{diff-reac}^n$.
- Truncation error is evaluated in a new variable $W(x)$.

$$\eta^n = \left\| W_h^{n-1}(X(x, \tau_n; \tau_{n-1})) - \overline{W}_h^{n-1}(x) \right\|_{L_2}^2 .$$

Numerical Method: Error estimation II

- For this problem the variable $W(x) = Z(x)$
- Truncation error:

$$\eta^n = \sum_K \left(\int_K \left[Z_h^{n-1}(X(x, \tau_n; \tau_{n-1})) - \overline{Z}_h^{n-1}(x) \right]^2 dK \right).$$

- We compute the integrals using quadrature points x_g.
  $x_g = F_K(\hat{x}_g)$ and $X^{n-1}(x_g) \approx y_g = \tilde{F}_K(\hat{x}_g)$.

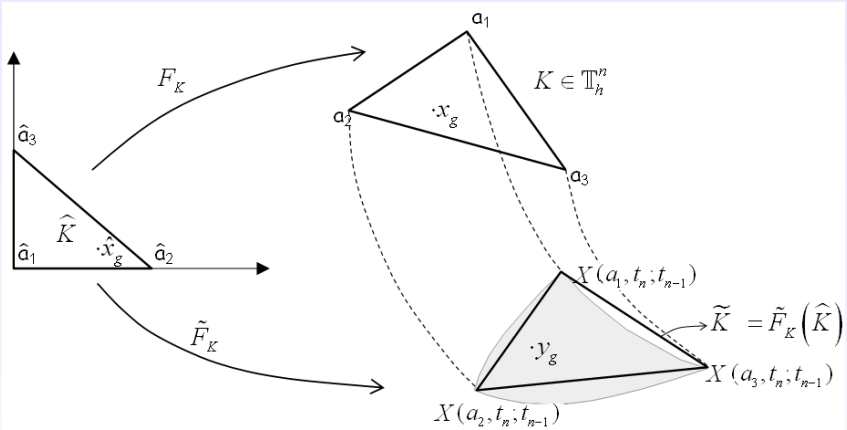

Numerical Method: Error estimation II

- For this problem the variable $W(x) = Z(x)$
- Truncation error:

$$\eta^n = \sum_K \left(\int_K \left[Z_h^{n-1}(X(x, \tau_n; \tau_{n-1})) - \overline{Z}_h^{n-1}(x) \right]^2 dK \right).$$

- We compute the integrals using quadrature points x_g.
  $x_g = F_K(\hat{x}_g)$ and $X^{n-1}(x_g) \approx y_g = \tilde{F}_K(\hat{x}_g)$.

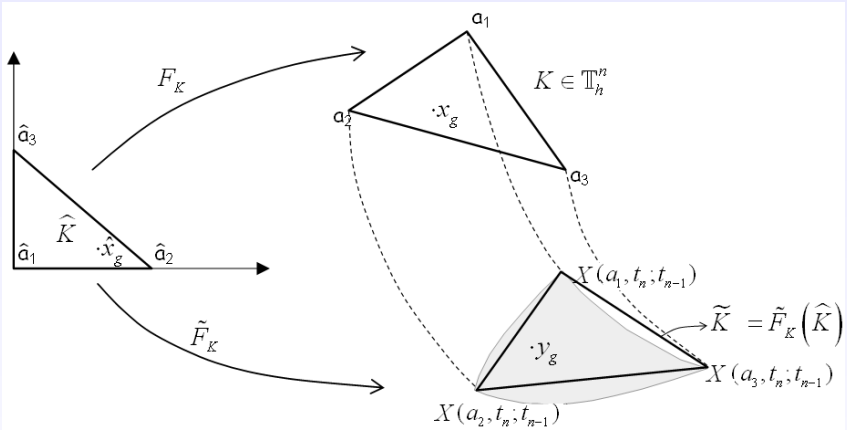

- The optimal size A_K^{opt} to satisfy $\eta^n < Tol$ is

$$A_K^{opt} = A_K \left(\frac{Tol}{\sum_{K \in \mathbb{T}_h} \eta_K^{1/(\alpha+1)}} \right)^{\frac{1}{\alpha}} \eta_K^{-1/(\alpha+1)} \quad \text{with} \quad \alpha = 3$$

Isotropic Adaptation: Bisection

The ratio A_K^{opt}/A_K defines the size of the new elements of the mesh.

Isotropic Adaptation: Bisection

The ratio A_K^{opt}/A_K defines the size of the new elements of the mesh.

- The element K (father) is divided into two elements (children) by cutting the refinement edge at its midpoint.
  Bisection algorithm

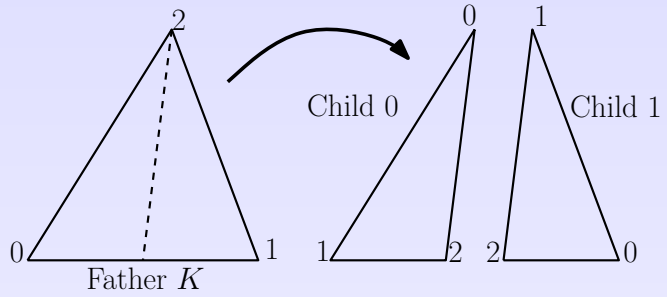

Isotropic Adaptation: Bisection

The ratio A_K^{opt}/A_K defines the size of the new elements of the mesh.

- The element K (father) is divided into two elements (children) by cutting the refinement edge at its midpoint.
  Bisection algorithm
- A conforming and non-degenerated triangulation must be always maintain.

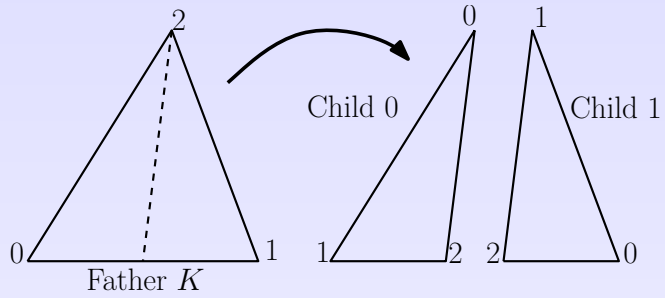

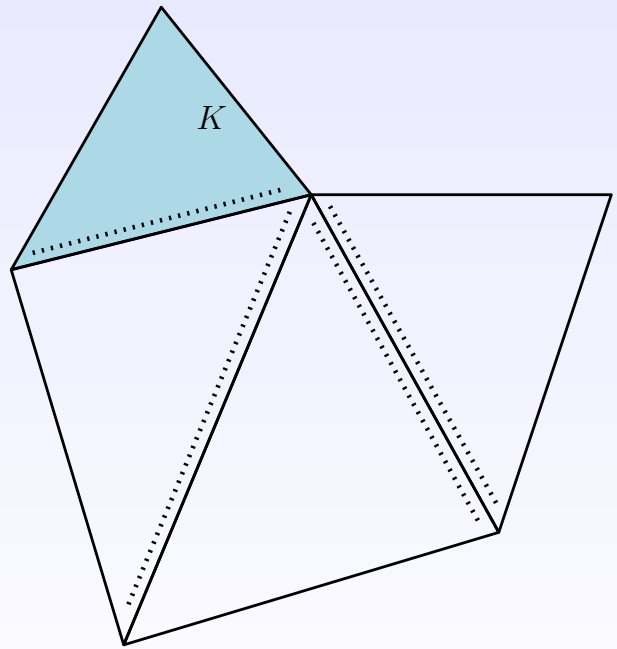

Isotropic Adaptation: Bisection

The ratio A_K^{opt}/A_K defines the size of the new elements of the mesh.

- The element K (father) is divided into two elements (children) by cutting the refinement edge at its midpoint.
  Bisection algorithm
- A conforming and non-degenerated triangulation must be always maintain.
  1. Avoid the presence of hanging nodes.

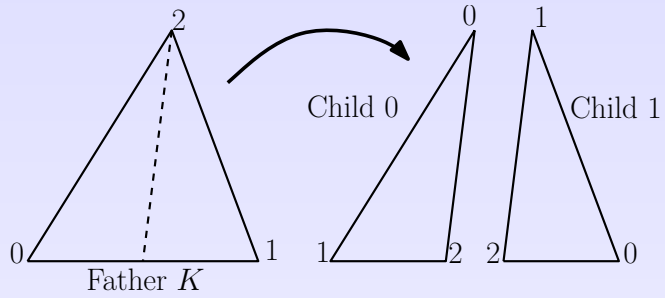

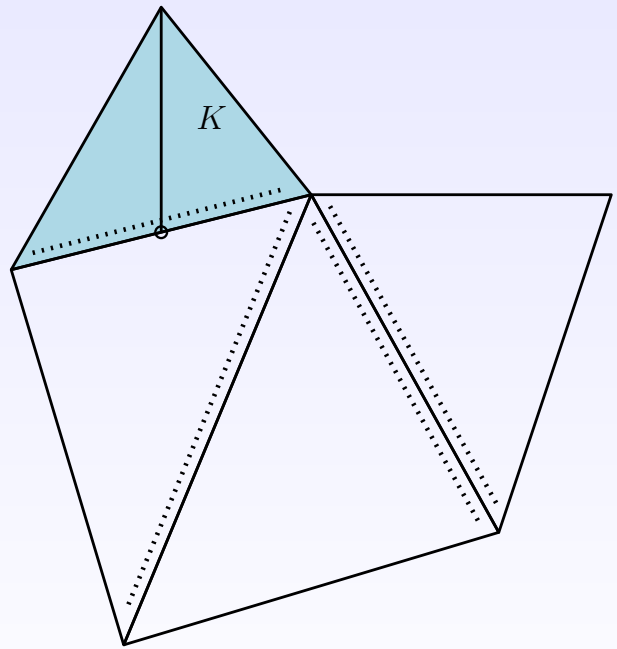

Isotropic Adaptation: Bisection

The ratio A_K^{opt}/A_K defines the size of the new elements of the mesh.

- The element K (father) is divided into two elements (children) by cutting the refinement edge at its midpoint.
  Bisection algorithm
- A conforming and non-degenerated triangulation must be always maintain.
  1. Avoid the presence of hanging nodes.
  2. Maintain the mesh regular in the refined procedure.

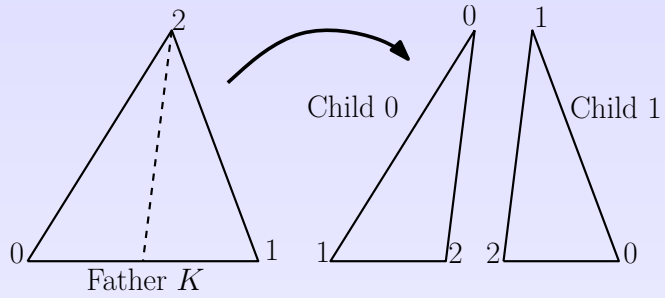

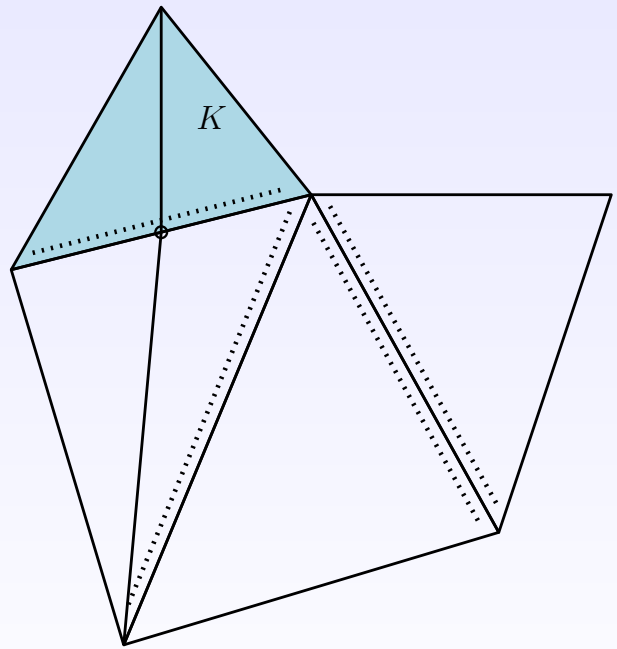

Isotropic Adaptation: Bisection

The ratio A_K^{opt}/A_K defines the size of the new elements of the mesh.

- The element K (father) is divided into two elements (children) by cutting the refinement edge at its midpoint.
  Bisection algorithm
- A conforming and non-degenerated triangulation must be always maintain.
  1. Avoid the presence of hanging nodes.
  2. Maintain the mesh regular in the refined procedure.
- A marked element forces to refine those elements which shear the refinement edge and only refinements by it are allowed.

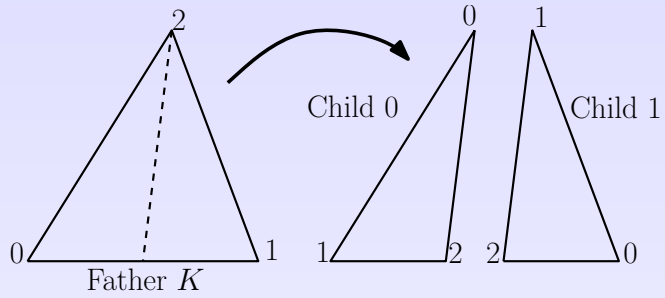

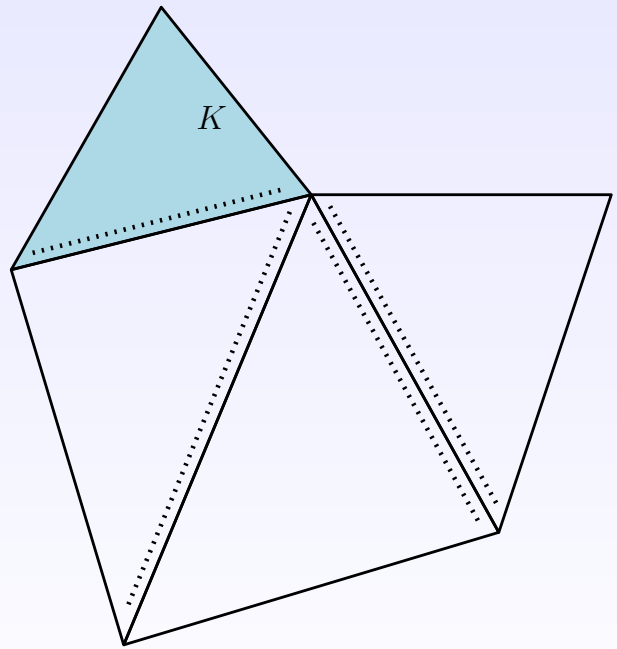

Isotropic Adaptation: Bisection

The ratio A_K^{opt}/A_K defines the size of the new elements of the mesh.

- The element K (father) is divided into two elements (children) by cutting the refinement edge at its midpoint.
  Bisection algorithm
- A conforming and non-degenerated triangulation must be always maintain.
  1. Avoid the presence of hanging nodes.
  2. Maintain the mesh regular in the refined procedure.
- A marked element forces to refine those elements which shear the refinement edge and only refinements by it are allowed.

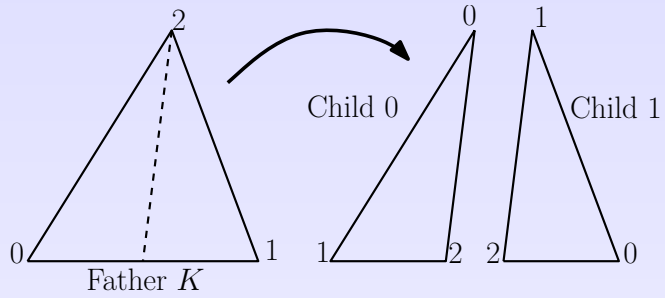

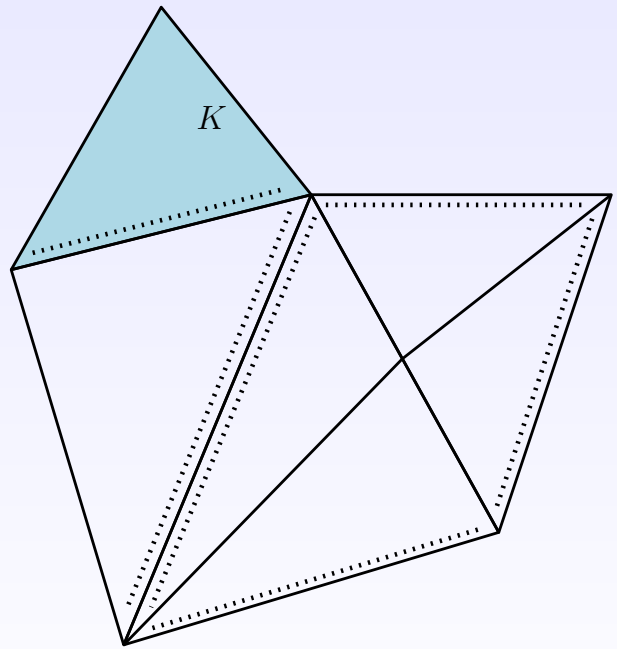

Isotropic Adaptation: Bisection

The ratio A_K^{opt}/A_K defines the size of the new elements of the mesh.

- The element K (father) is divided into two elements (children) by cutting the refinement edge at its midpoint.
  Bisection algorithm
- A conforming and non-degenerated triangulation must be always maintain.
  1. Avoid the presence of hanging nodes.
  2. Maintain the mesh regular in the refined procedure.
- A marked element forces to refine those elements which shear the refinement edge and only refinements by it are allowed.

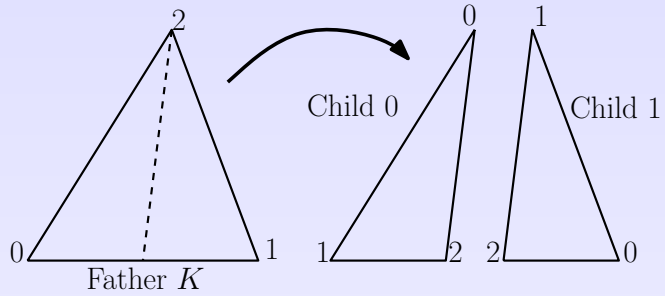

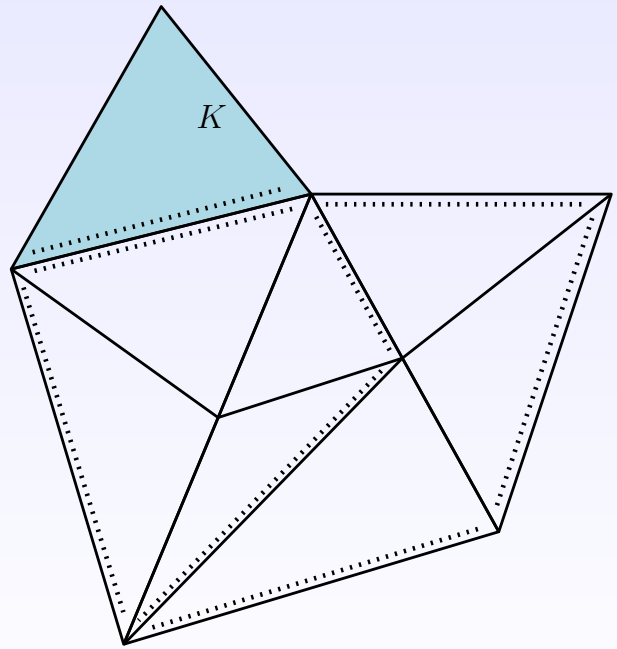

Isotropic Adaptation: Bisection

The ratio A_K^{opt}/A_K defines the size of the new elements of the mesh.

- The element K (father) is divided into two elements (children) by cutting the refinement edge at its midpoint.
  Bisection algorithm
- A conforming and non-degenerated triangulation must be always maintain.
  1. Avoid the presence of hanging nodes.
  2. Maintain the mesh regular in the refined procedure.
- A marked element forces to refine those elements which shear the refinement edge and only refinements by it are allowed.

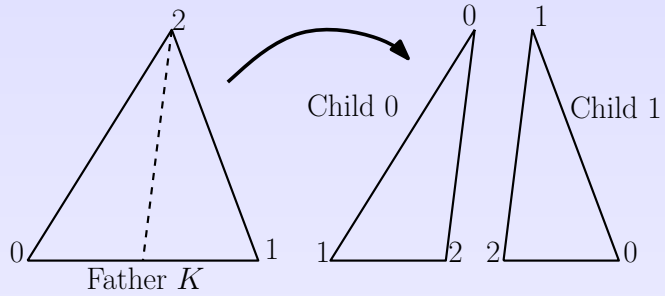

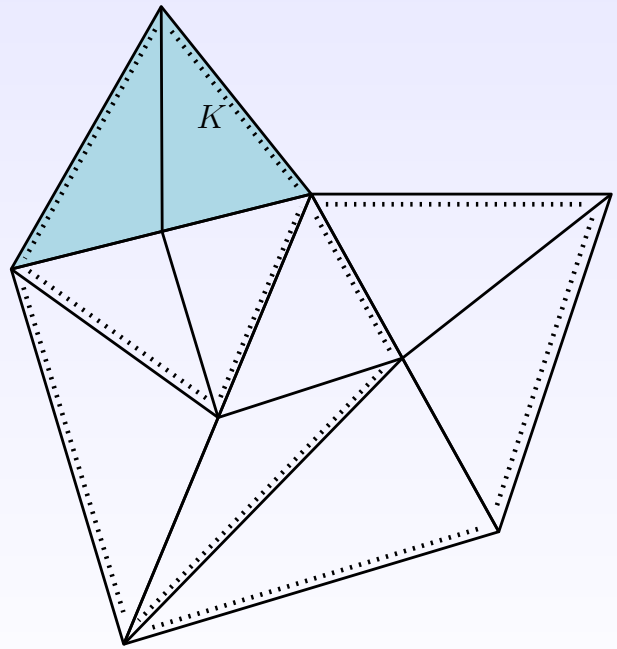

Isotropic Adaptation: 2D

- In 2D the refinement loop finishes if the refinement edge is the longest edge of each element.

Isotropic Adaptation: 2D

- In 2D the refinement loop finishes if the refinement edge is the longest edge of each element.

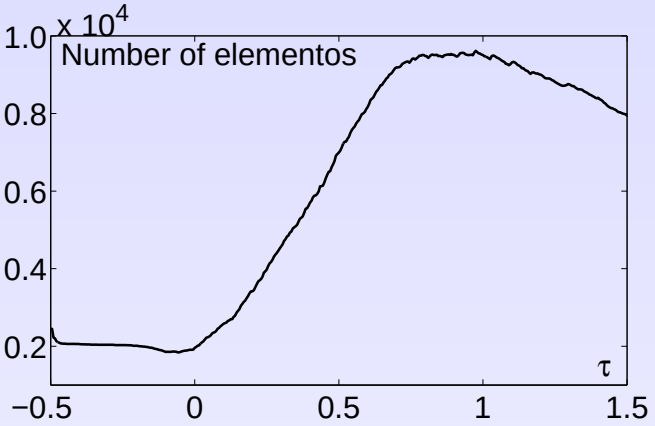

(Loading...)

(Loading...)

$$Pe_0 = 80, \quad \widetilde{\Gamma} = 40$$

Isotropic Adaptation: 3D

- In 3D the refinement loop is more complicated.

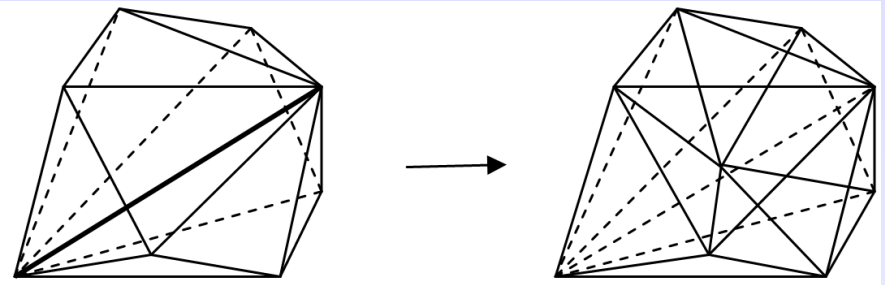

- The loop finishes if the macro-triangulation satisfies the Kossaczky condition (The mesh is derived form hexahedral triangulation and they are classified in 3 types of elements):

  I.Kossaczky. Journal of Computational and Applied Mathematics (1994).

  1. An arbitrary mesh needs a pre-adaptation divided each tetrahedron into twelve tetrahedra.
  2. Use a mesh generator satisfying the required conditions:

     R. Montenegro, J.M. Cascón, J.M. Escobar, E. Rodrǵuez, G. Montero. Institute for Intelligent Systems and Numerical Applications in Engineering (2009).

Isotropic Adaptation: 3D

Tridimensional simulations

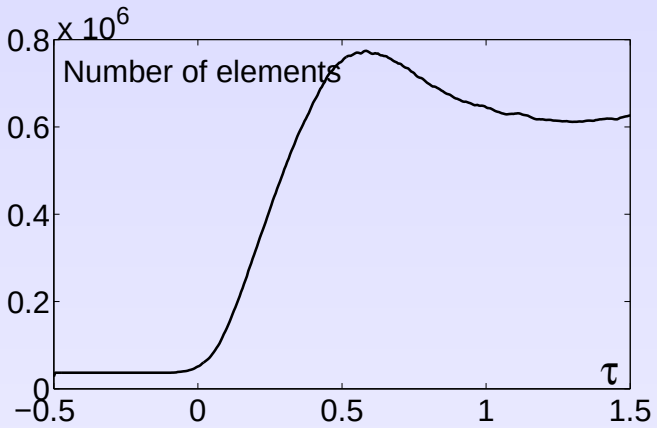

(Loading...)

(Loading...)

$$Pe_0 = 80, \quad \widetilde{\Gamma} = 40$$

Anisotropic versus Isotropic Adaptation: 2D

- With the bisection algorithm mesh elements are adjusted only in size.
- In some cases the solution shows directional features.
- In these situations, anisotropic meshes might provide better results.

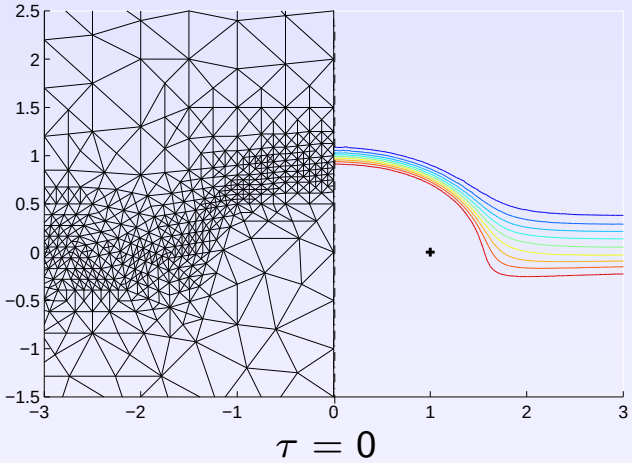

$\tau = 0$

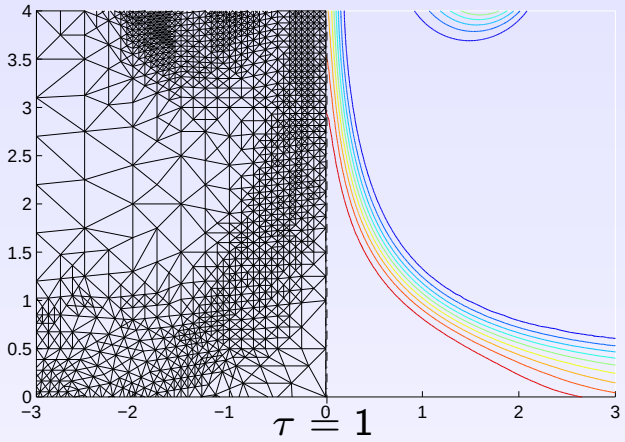

$\tau = 1$

Anisotropic versus Isotropic Adaptation: 2D

- With the bisection algorithm mesh elements are adjusted only in size.
- In some cases the solution shows directional features.
- In these situations, anisotropic meshes might provide better results.

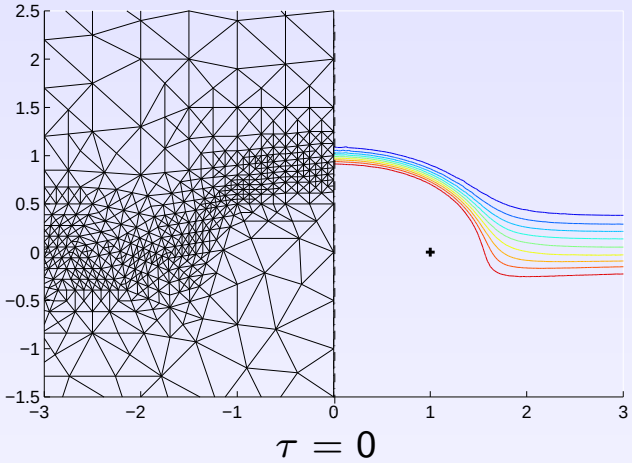

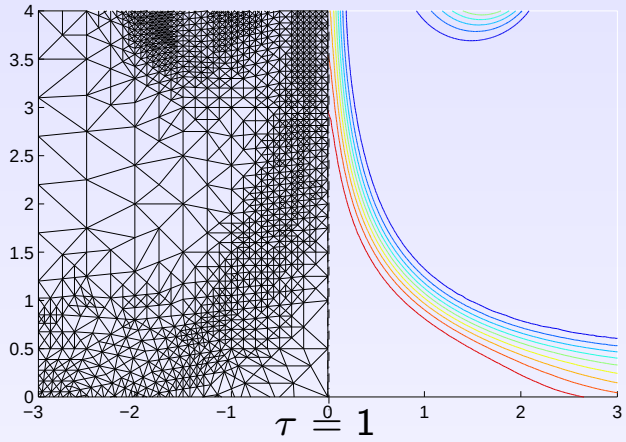

- The size but also the shape and orientation of the mesh must be defined. Metric tensor.

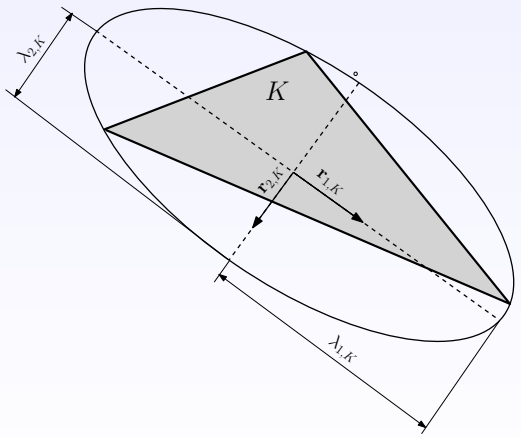

Anisotropic Adaptation: 2D

The metric tensor parameters depend on the a posteriori error estimator:

$$\|Z - I_K(Z)\|_{L^2(K)} \leq C\,|K| \left[\sum_{i=1}^{d} s_{i,K} \left(\mathbf{r}_{i,K}^T G_K(Z) \mathbf{r}_{i,K}\right)\right]^{1/2}$$

with $G(Z)$ Hessian matrix of the solution Z where $\lambda_{i,K} = s_{i,K}\ |K|^{1/d}$

Anisotropic Adaptation: 2D

The metric tensor parameters depend on the a posteriori error estimator:

$$\|Z - I_K(Z)\|_{L^2(K)} \leq C\,|K| \left[\sum_{i=1}^{d} s_{i,K}\left(\mathbf{r}_{i,K}^T G_K(Z)\mathbf{r}_{i,K}\right)\right]^{1/2}$$

with $G(Z)$ Hessian matrix of the solution Z where $\lambda_{i,K} = s_{i,K}\,|K|^{1/d}$

- The optimal shape and orientation of the triangle are given by:

$$\begin{aligned} \hat{s}_{i,k} &= \left(\prod_{i=1}^{d} g_{i,K}\right)^{1/d} g_{d+1-i,K}^{-1} \\ \hat{\mathbf{r}}_{i,K}^T &= \mathbf{l}_{d+1-i,K} \end{aligned}$$

  where $\mathbf{l}_i$ and $g_{i,K}$ is the eigenvector and eigenvalue of the Hessian matrix $G(Z)$.

- The size of the triangles is given by A_K^{opt} computed before.

- Mesh generator code used in this work:

  F. Hecht, 'BAMG: Bidimensional Anisotropic Mesh Generator'

Anisotropic Adaptation: 2D

Simulation with anisotropic elements: Axisymmetric configuration

(Loading...)

(Loading...)

$$Pe_0 = 80, \quad \widetilde{\Gamma} = 40$$

Anisotropic Adaptation: 2D

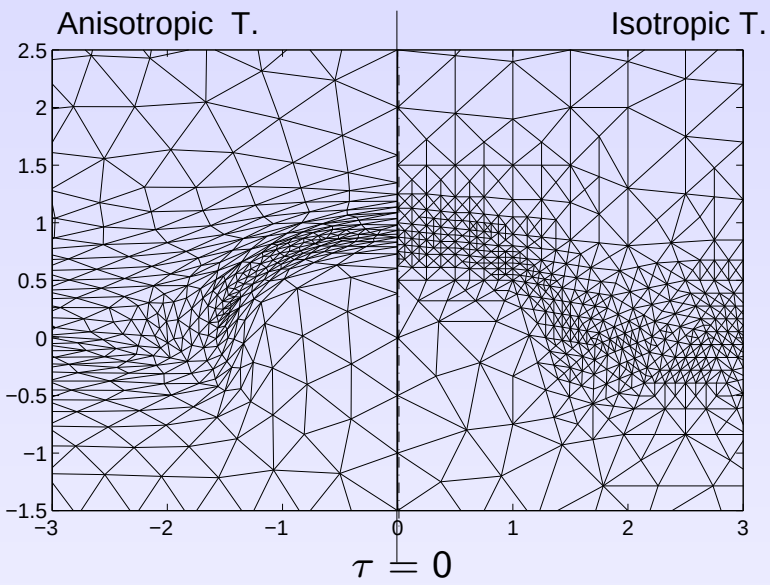

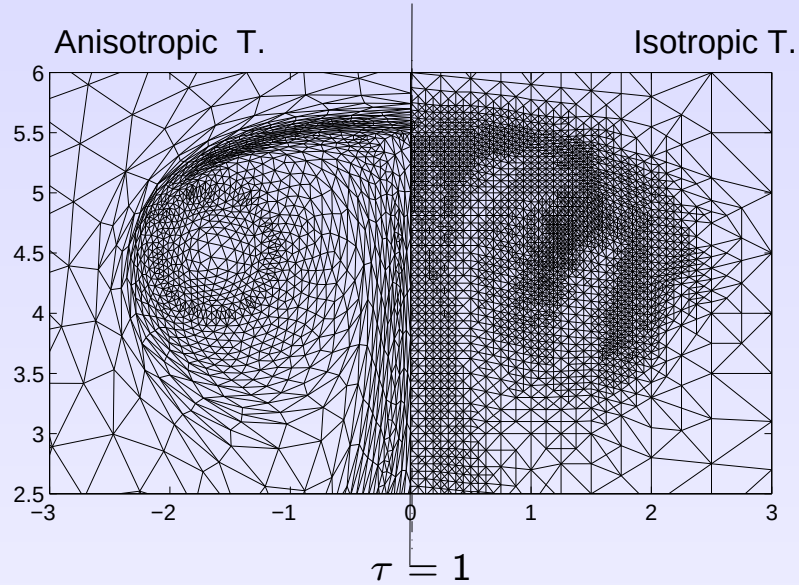

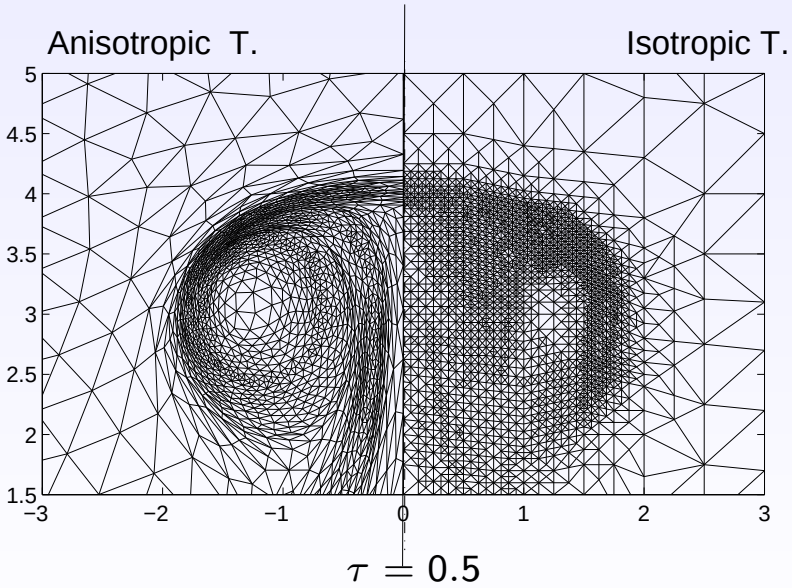

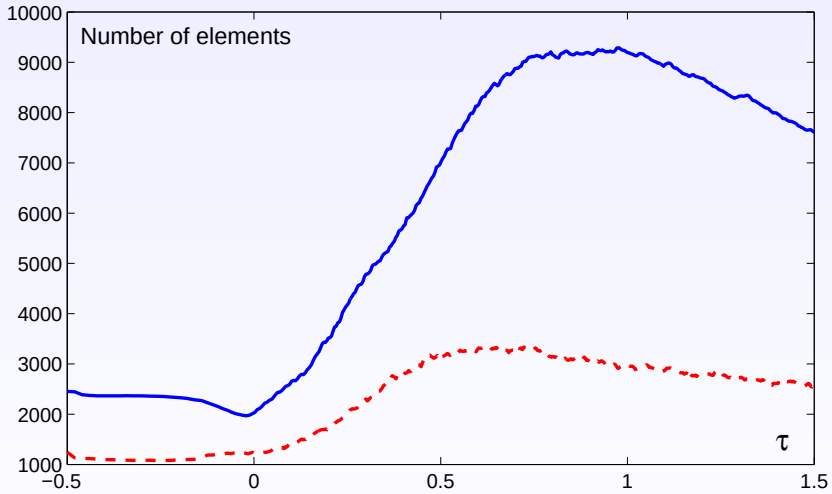

Model II

- Model II (Complex model)
  - Detailed transport models.
  - H_2/Air chemical kinetic model.

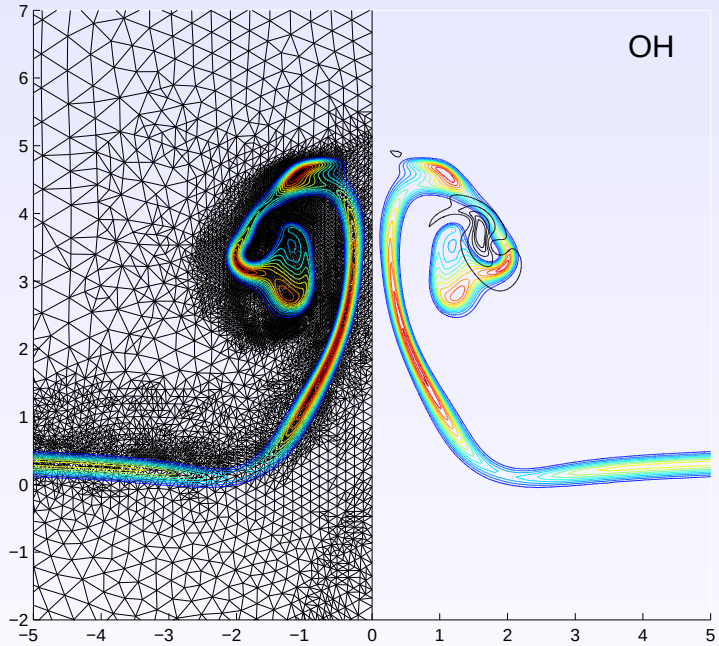

Model II: Constitutive Equations

$$\rho = \frac{M}{T}, \qquad M = \frac{1}{M_A}\left(\sum_{i=1}^{I} Y_i/M_i\right)^{-1}$$

$$\mathbf{q} = -\lambda \nabla T + \sum_{i=1}^{I} h_i \mathbf{j}_i, \qquad \lambda = \frac{\lambda' T_0}{\rho_A D_{TA} h_A}, \qquad h_i = h_i'/h_A$$

$$\mathbf{j}_i = \rho Y_i \left(\mathbf{V}_i^D + \mathbf{V}_i^T + \mathbf{V}_c\right), \qquad \rho D_i = \frac{\rho' D_i'}{\rho D_{TA}}$$

Ordinary diffusion $\quad \mathbf{V}_i^D = -\frac{D_i}{X_i}\nabla X_i$

Thermal diffusion $\quad \mathbf{V}_i^T = \frac{D_i \theta_i}{X_i}\frac{\nabla T}{T}$

Correction velocity $\quad \mathbf{V}_c = -\sum \left(Y_i \mathbf{V}_i^D + Y_i \mathbf{V}_i^T\right)$

where h_i', μ', λ', D_i' and θ_i are functions of the local thermodynamical state of the mixture (Kee et al., CHEMKIN (1983)).

Model II: Chemistry Model

$$\dot{m}_i = \frac{\dot{m}'_i}{\rho_A A_{ext}}$$

$$3H_2 + O_2 \overset{\text{I}}{\rightleftharpoons} 2H + 2H_2O$$

$$2H \overset{\text{II}}{\rightleftharpoons} H_2$$

Reaction		A	n	$T_a[K]$
1. $H+O_2 \rightleftharpoons OH+O$	k_f	$3.52 \cdot 10^{16}$	-0.700	8590
	k_b	$7.04 \cdot 10^{13}$	-0.264	72
2. $H_2+O \rightleftharpoons OH+H$	k_f	$5.06 \cdot 10^{4}$	2.670	3166
	k_b	$3.03 \cdot 10^{4}$	2.633	2433
3. $H_2+OH \rightleftharpoons H_2O+H$	k_f	$1.17 \cdot 10^{9}$	1.300	1829
	k_b	$1.29 \cdot 10^{10}$	1.196	9412
4. $H+O_2+M_4 \rightarrow HO_2+M_4$	k_0	$5.75 \cdot 10^{19}$	-1.400	0
	k_∞	$4.65 \cdot 10^{12}$	0.440	0
5f. $HO_2+H \rightarrow OH+OH$		$7.08 \cdot 10^{13}$	0	148
6. $HO_2+H \rightarrow H_2+O_2$	k_f	$1.66 \cdot 10^{13}$	0	414
	k_b	$2.69 \cdot 10^{12}$	0.36	27888
7. $HO_2+OH \rightarrow H_2O+O_2$		$2.89 \cdot 10^{13}$	0	-250
8. $H+OH+M_8 \rightarrow H_2O+M_8$	k_f	$4.00 \cdot 10^{22}$	-2.0	0
	k_b	$1.03 \cdot 10^{23}$	-1.75	59675
9. $H+H+M_9 \rightarrow H_2+M_9$	k_f	$1.30 \cdot 10^{18}$	-1.0	0
	k_b	$3.04 \cdot 10^{17}$	-0.65	52092

San Diego Mechanism (2005)

$$w'_{\text{I}} = k_{1f} C_{O_2} C_H - k_{1b} C_{OH} C_O + k_{5f} C_H C_{HO_2}$$
$$w'_{\text{II}} = k_{4f} C_{M_4} C_{O_2} C_H + k_{8f} C_{M_8} C_H C_{OH} + k_{9f} C_{M_9} C_H C_H$$

Mauss et al. (1993)

Model II: Boundary Conditions

Boundary conditions are taken from the steady unperturbed counterflow configuration

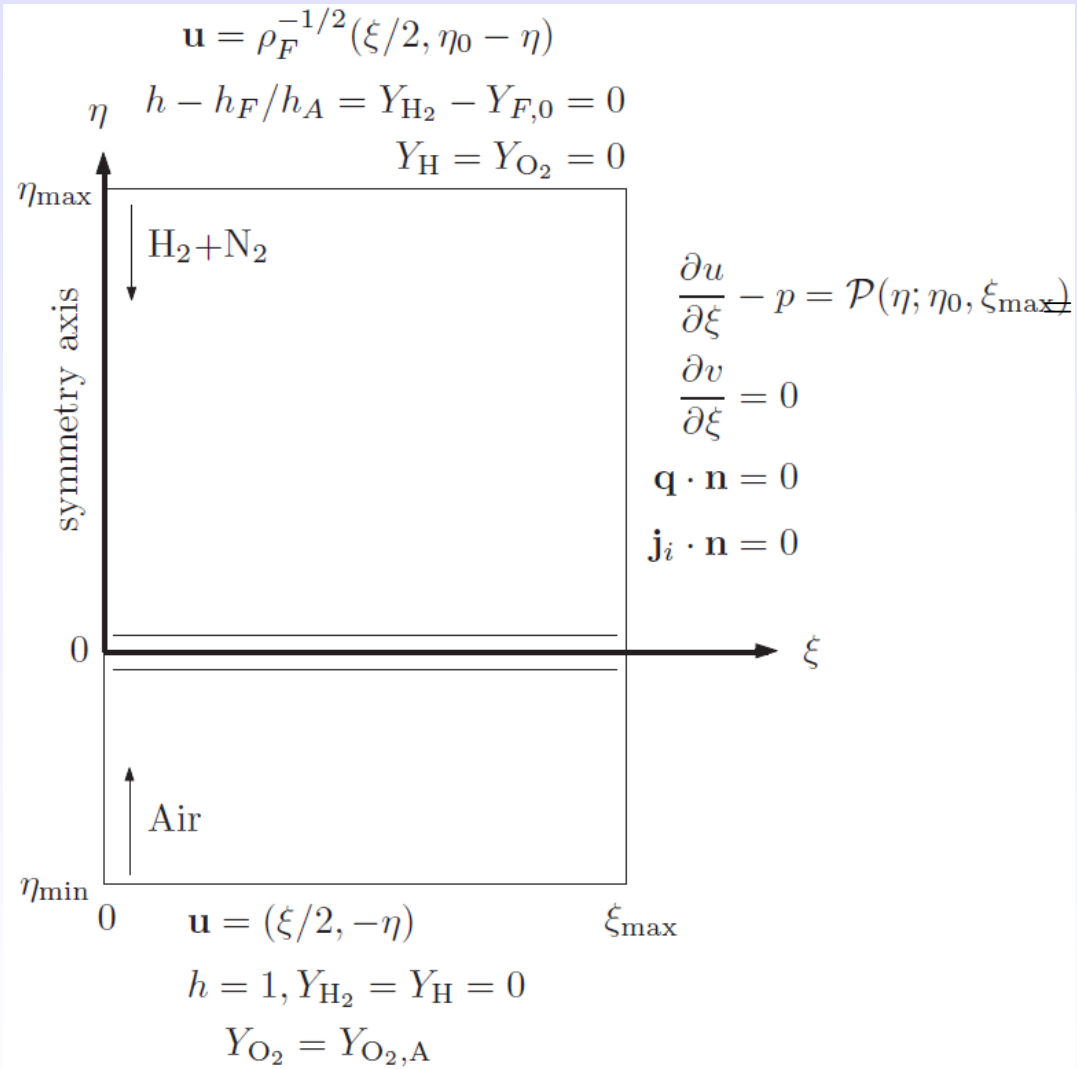

$$\begin{cases} \xi_{max}^2/8 + (\eta - \eta_0)^2/2 & \eta_0 < \eta, \\ \xi_{max}^2/8 & 0 < \eta < \eta_0, \\ \xi_{max}^2/8 + \eta^2/2 & \eta < 0. \end{cases}$$

Model II: Initial Conditions

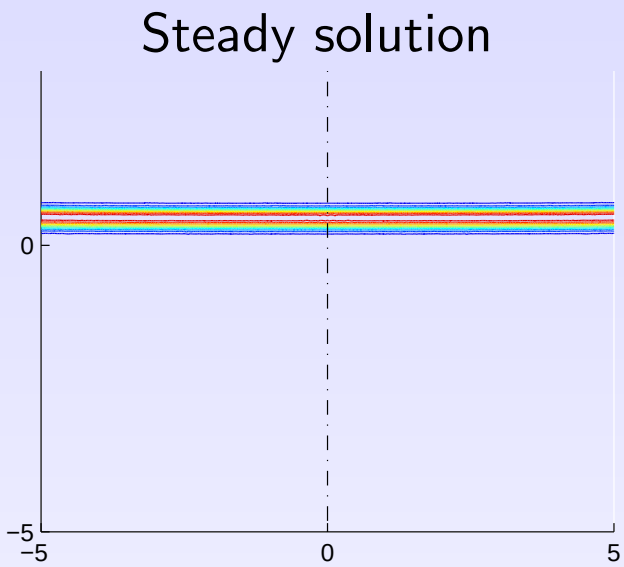

$$u = u_{ss}$$

$$v = v_{ss}$$

Model II: Initial Conditions

Steady solution + vortex ring

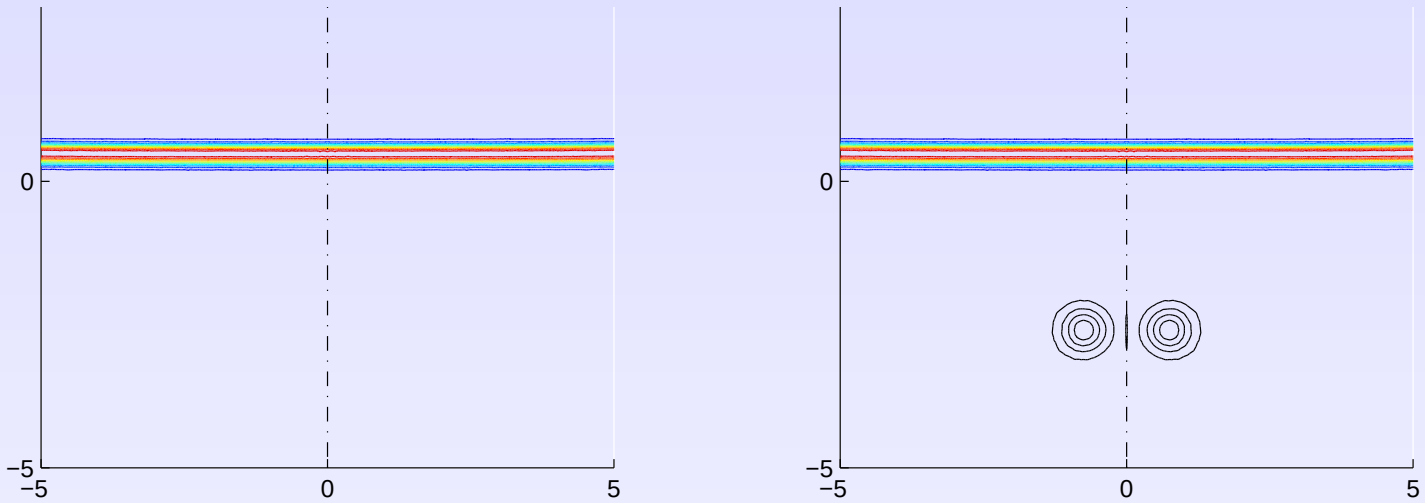

$$u = u_{ss} - \frac{\widetilde{\Gamma}}{\pi \xi_c} \left(\frac{\xi_c}{2\xi} \right)^{3/2} \left(\frac{\eta - \eta_c}{\xi_c} \right) I_1(\mu) \left[1 - \mathrm{e}^{-(\rho/\delta_v)^2} \right]$$

$$v = v_{ss} + \frac{\widetilde{\Gamma}}{\pi \xi_c} \left(\frac{\xi_c}{2\xi} \right)^{3/2} \left[\frac{\xi}{\xi_c} I_1(\mu) - I_0(\mu) \right] \left[1 - \mathrm{e}^{-(\rho/\delta_v)^2} \right]$$

$$\widetilde{\Gamma} = \Gamma / \left(2 A_0 r_0^2 \right)$$

Hermanns et al., Combustion & Flame (2007)

Numerical Method: Compute the numerical solution

- Navier-Stokes and energy-mass conservation can be written as:

$$\rho\left(\frac{\partial c}{\partial \tau} + \mathbf{u}\cdot\nabla c\right) = \nabla\cdot\mathbf{f}(c) \qquad \textit{in } \Omega\times(\tau_{n-1},\tau_n]$$

Numerical Method: Compute the numerical solution

- Navier-Stokes and energy-mass conservation can be written as:

$$\rho\left(\frac{\partial c}{\partial \tau} + \mathbf{u}\cdot\nabla c\right) = \nabla\cdot\mathbf{f}(c) \qquad in\ \Omega\times(\tau_{n-1},\tau_n]$$

- They can be uncoupled using a Semi-Lagrangian scheme to treat convective terms (only $\mathbf{u}^{n-1}, \mathbf{u}^{n-2}$ are needed)

$$\rho^*\frac{\partial c^*}{\partial \tau} = \nabla^*\cdot\mathbf{f}(c^*) \qquad in\ \Omega\times(\tau_{n-1},\tau_n]$$

Numerical Method: Compute the numerical solution

- Navier-Stokes and energy-mass conservation can be written as:

$$\rho\left(\frac{\partial c}{\partial \tau} + \mathbf{u}\cdot\nabla c\right) = \nabla\cdot\mathbf{f}(c) \qquad in\ \Omega\times(\tau_{n-1},\tau_n]$$

- They can be uncoupled using a Semi-Lagrangian scheme to treat convective terms (only $\mathbf{u}^{n-1}, \mathbf{u}^{n-2}$ are needed)

$$\rho^*\frac{\partial c^*}{\partial \tau} = \nabla^*\cdot\mathbf{f}(c^*) \qquad in\ \Omega\times(\tau_{n-1},\tau_n]$$

1. Energy-mass equations are solved with an explicit Runge-Kutta Chebyshev (RCK) scheme in time (second order) and P_2 in space. h^n, Y_i^n and from them T^n.

Bermejo & Carpio, Appl. Num. Math. (2008)

Numerical Method: Compute the numerical solution

- Navier-Stokes and energy-mass conservation can be written as:

$$\rho\left(\frac{\partial c}{\partial \tau} + \mathbf{u}\cdot\nabla c\right) = \nabla\cdot\mathbf{f}(c) \qquad in\ \Omega\times(\tau_{n-1},\tau_n]$$

- They can be uncoupled using a Semi-Lagrangian scheme to treat convective terms (only $\mathbf{u}^{n-1}, \mathbf{u}^{n-2}$ are needed)

$$\rho^*\frac{\partial c^*}{\partial \tau} = \nabla^*\cdot\mathbf{f}(c^*) \qquad in\ \Omega\times(\tau_{n-1},\tau_n]$$

1. Energy-mass equations are solved with an explicit Runge-Kutta Chebyshev (RCK) scheme in time (second order) and P_2 in space. h^n, Y_i^n and from them T^n.

   Bermejo & Carpio, Appl. Num. Math. (2008)

2. Navier-Stokes is solved with a BDF scheme of 2^o order in time and Taylor-Hood P_2/P_1 in space. $\mathbf{u}^n$ and p^n.

- The error indicator η^n is measure for:

$$W(c) = 10^3\,Y_H + 10^{-3}(u^2+v^2)$$

Validation: Steady-State Extinction Curves

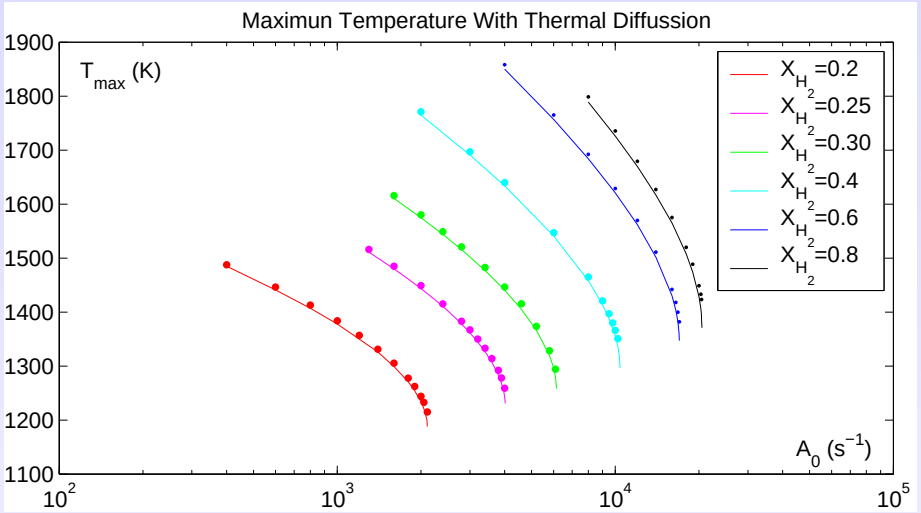

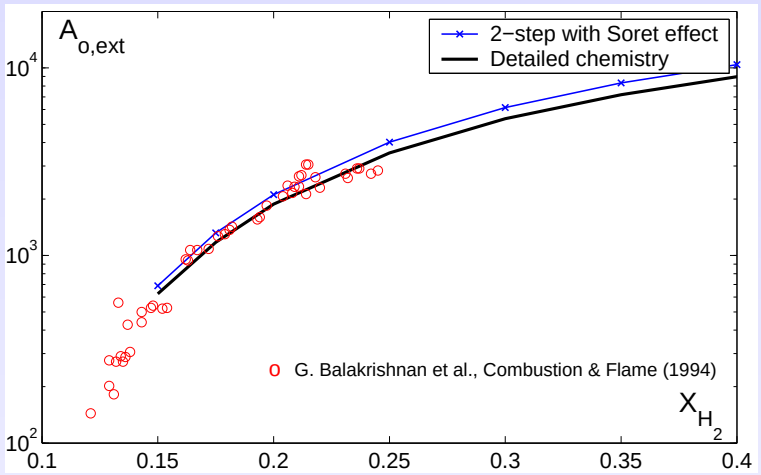

- We compute the steady-state counterflow configuration
  - The steady solutions are used as initial conditions for the unsteady calculations
  - The numerical solution is validated with COSILAB

Validation: Steady-State Extinction Curves

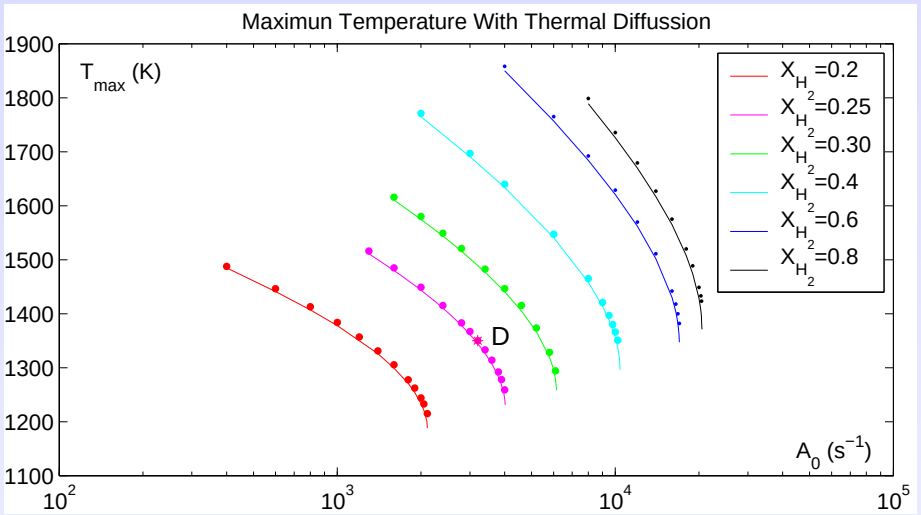

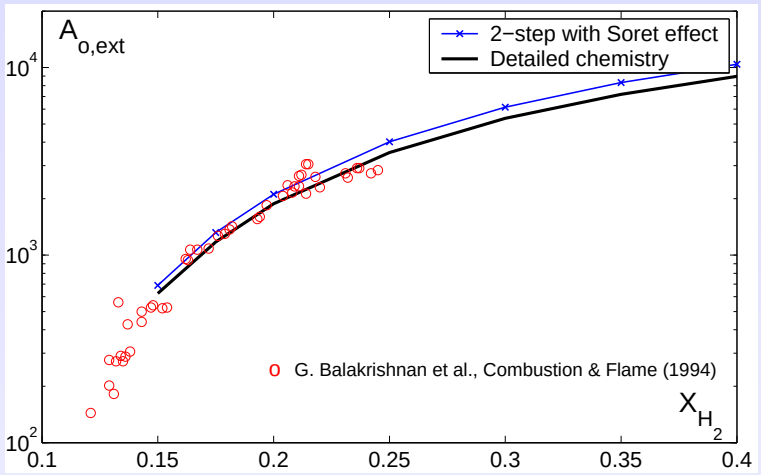

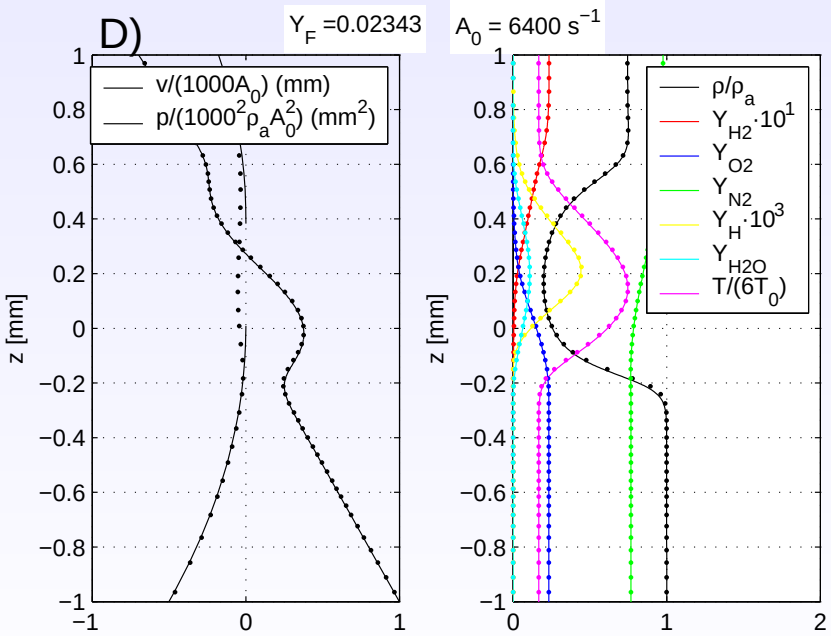

Validation: Steady-State Extinction Curves

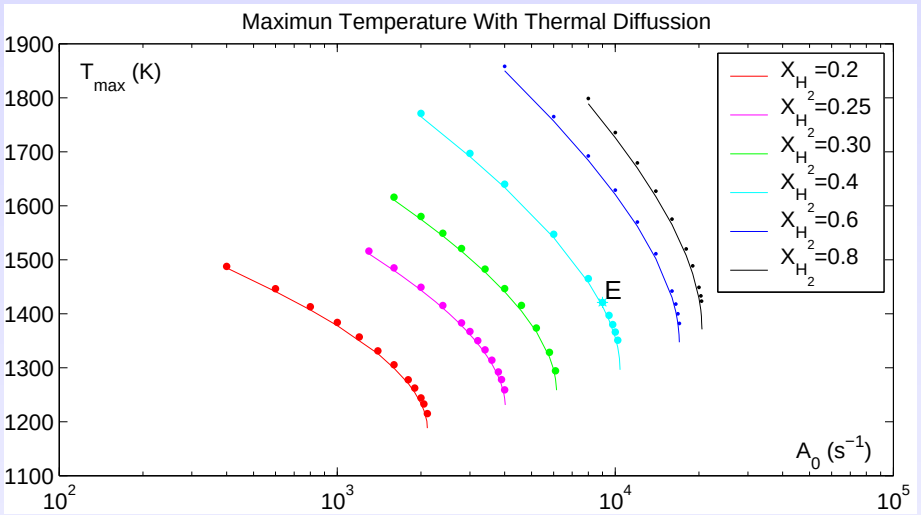

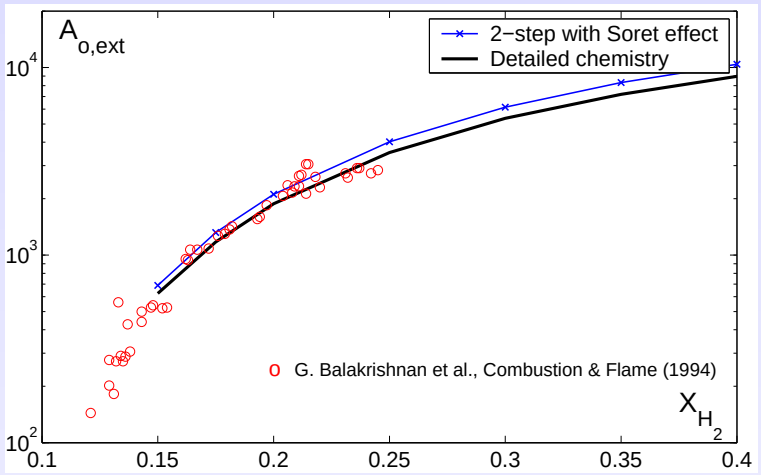

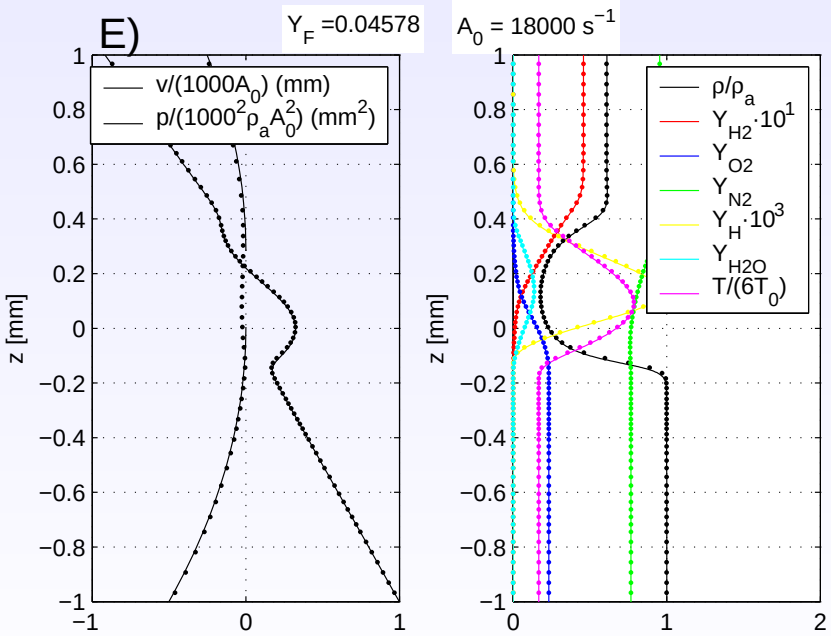

Validation: Steady-State Extinction Curves

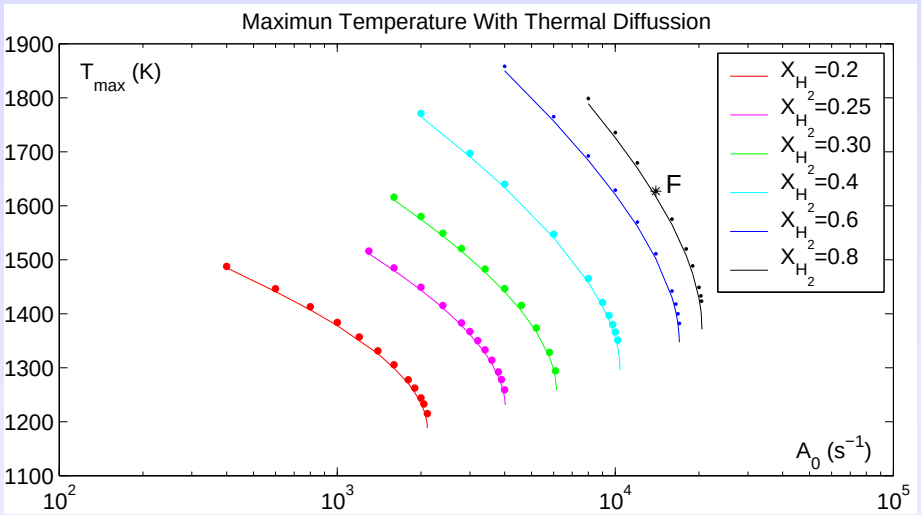

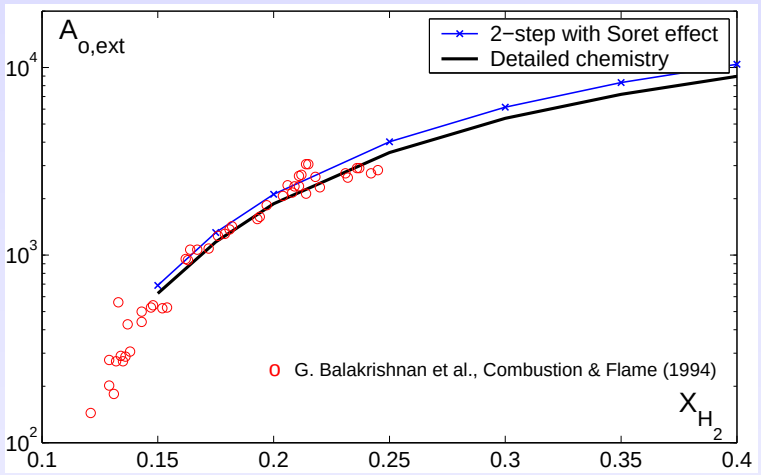

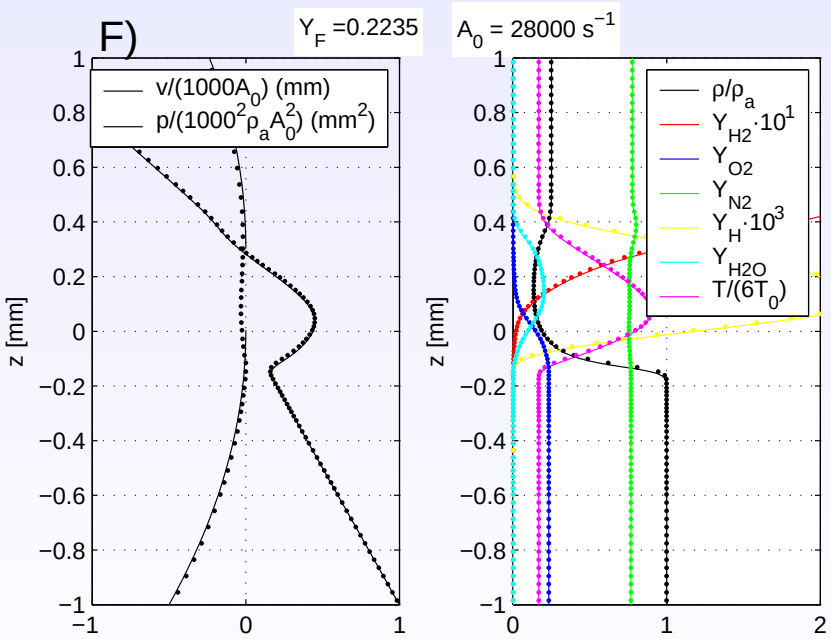

Numerical Results: Case 1

Renard et al., Combustion & Flame (1999)

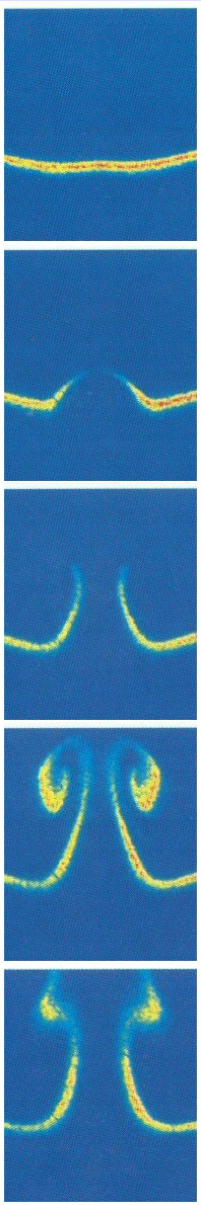

$$Y_{F0} = 0.015 \quad \rightarrow \quad A_{ext} = 1300 s^{-1}$$

$$Pe_0 = 30, \quad \widetilde{\Gamma} = 33, \quad \mathcal{R} = 30$$

Numerical Results: Case 1

Renard et al., Combustion & Flame (1999)

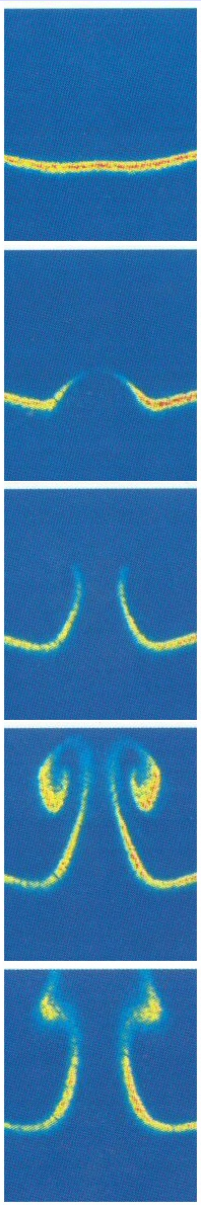

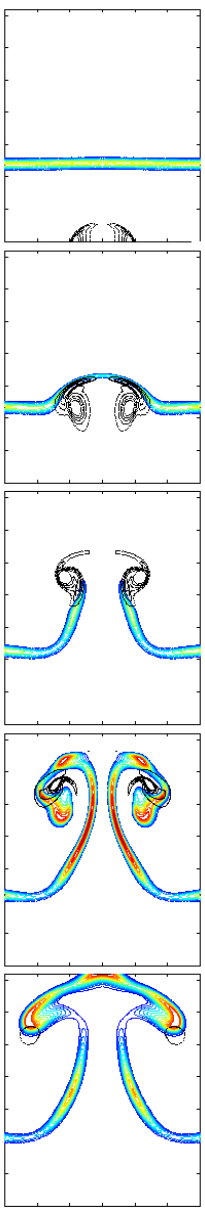

Carpio et al., 2011

(Loading...)

$$Y_{F0} = 0.015 \quad \rightarrow \quad A_{ext} = 1300 s^{-1}$$

$$Pe_0 = 30, \quad \widetilde{\Gamma} = 33, \quad \mathcal{R} = 30$$

Numerical Results: Case 2

Renard et al., Combustion & Flame (1999)

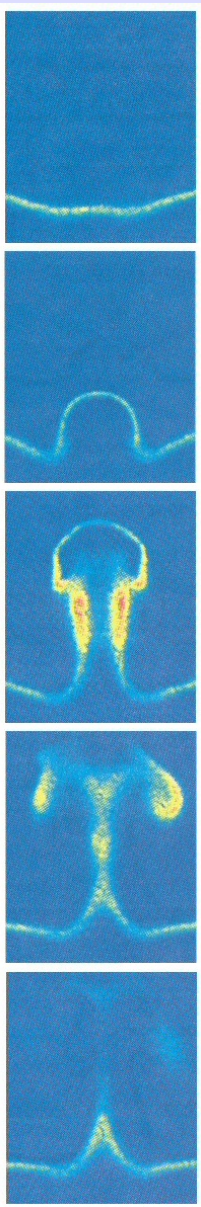

Carpio et al., 2011

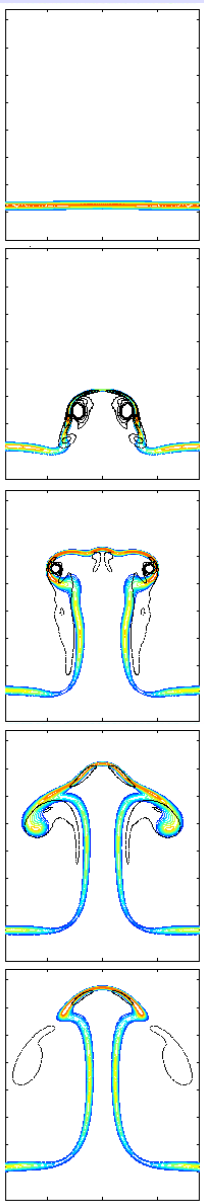

(Loading...)

$$Y_{F0} = 0.02 \quad \rightarrow \quad A_{ext} = 3200 s^{-1}$$

$$Pe_0 = 60, \quad \widetilde{\Gamma} = 35, \quad \mathcal{R} = 45$$

Numerical Results: Case 3

Renard et al., Combustion & Flame (1999)

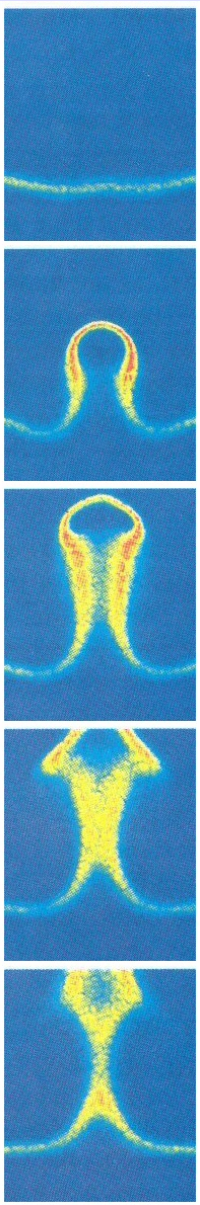

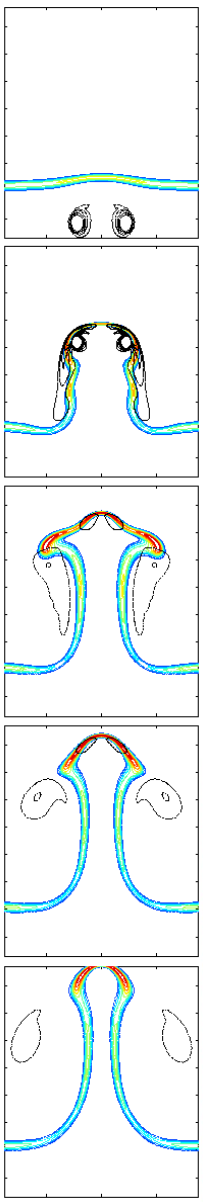

Carpio et al., 2011

(Loading...)

$$Y_{F0} = 0.029 \quad \rightarrow \quad A_{ext} = 6000 s^{-1}$$

$$Pe_0 = 40, \quad \widetilde{\Gamma} = 40, \quad \mathcal{R} = 100$$

Conclusions

Conclusions

- A novel space-adaptive finite element algorithm has been used to simulate diluted hydrogen-air diffusion-flame/vortex interactions.
- Two different mathematical models have been used here.

Model I(Simple model)

- This model assumes constant physical coefficients and infinitely robust flames.
- This model allows us to analyze several refinement strategies. Anisotropic adaptation shows the better behavior.

Model II(Complex model)

- The mathematical model accounts detailed transport (CHEMKIM approach) and assumes a two-step reduced kinetic mechanism for hydrogen-air combustion.
- The results have been validated quantitatively using steady-state extinction curves and qualitatively against previously published experimental results.

INDUSTRIALES
ETSII | UPM

E.T.S. Ingenieros Industriales
Universidad Politécnica de Madrid

Ideas to create an adaptive finite element method for combustion problems

Jaime Carpio Huertas

A jointly work with:

Professors:
Rodolfo Bermejo
Marcos Vera
Miguel Hermanns
Amable Liñán

Students:
Pablo Fraile
Ángel Fernández

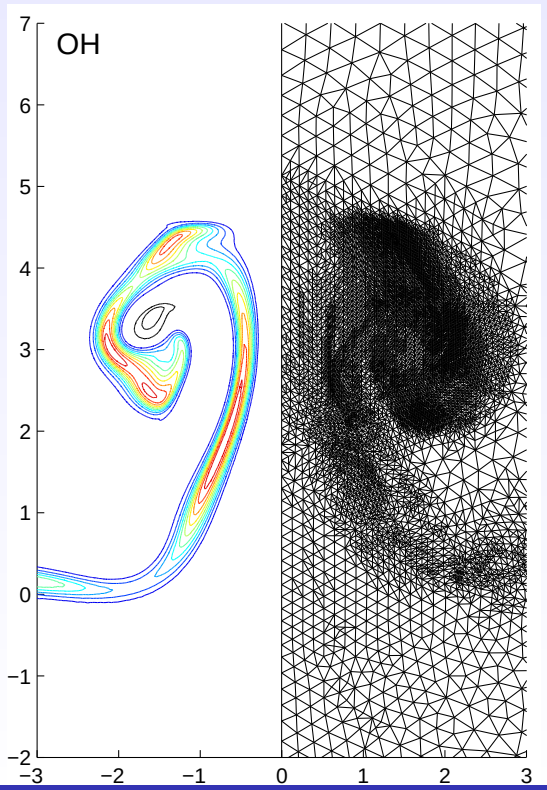

Workshop on mathematical modelling of combustion
23-25/05/2011